Austrian Journal of Technical and Natural Sciences

№ 3–4 2020
March – April

PREMIER
Publishing

Vienna
2020

Austrian Journal of Technical and Natural Sciences

Scientific journal
№ 3–4 2020 (March – April)

ISSN 2310-5607

Editorial office Premier Publishing s.r.o.
Praha 8 – Karlín, Lyčkovo nám. 508/7, PSČ 18600

E-mail: pub@ppublishing.org

Homepage: ppublishing.org

Austrian Journal of Technical and Natural Sciences is an international, German/English/Russian language, peer-reviewed journal. It is published bi-monthly with circulation of 1000 copies.

The decisive criterion for accepting a manuscript for publication is scientific quality. All research articles published in this journal have undergone a rigorous peer review. Based on initial screening by the editors, each paper is anonymized and reviewed by at least two anonymous referees. Recommending the articles for publishing, the reviewers confirm that in their opinion the submitted article contains important or new scientific results.

Premier Publishing s.r.o. is not responsible for the stylistic content of the article. The responsibility for the stylistic content lies on an author of an article.

Instructions for authors

Full instructions for manuscript preparation and submission can be found through the Premier Publishing s.r.o. home page at:
http://ppublishing.org.

Material disclaimer

The opinions expressed in the conference proceedings do not necessarily reflect those of the Premier Publishing s.r.o., the editor, the editorial board, or the organization to which the authors are affiliated.

Premier Publishing s.r.o. is not responsible for the stylistic content of the article. The responsibility for the stylistic content lies on an author of an article.

Included to the open access repositories:

ULRICHSWEB™ GLOBAL SERIALS DIRECTORY · НАУЧНАЯ ЭЛЕКТРОННАЯ БИБЛИОТЕКА eLIBRARY.RU · CYBERLENINKA · Google scholar

Typeset in Berling by Ziegler Buchdruckerei, Linz, Austria.
Printed by Premier Publishing s.r.o., Vienna, Austria on acid-free paper.

Section 1. Technical sciences

https://doi.org/10.29013/AJT-20-3.4-3-9

Rakhimov Dilshod Pulatovich,
Tashkent chemical-technological institute, Uzbekistan
E-mail: rahimov1984@list.ru

Abdullaev Utkir Saidakbar ugli,
Tashkent chemical-technological institute, Uzbekistan
E-mail: abdullaev_utkir@list.ru

Rakhimov Pulat Hadjievich,
Urganch State University, Uzbekistan
E-mail: muslimdilshod@mail.ru

Ruzibaev Akbarali Tursunbaevich,
Tashkent chemical-technological institute, Uzbekistan
E-mail: akbar216@mail.ru

GETTING A MODIFIED INTERESTERIFICATION USING THE COMBINATION OF LIQUID OILS AND SOLID FAT

Abstract. The aim of this work is to develop modified transesterifications with a reduced trans-acid content as local raw materials using liquid vegetable sunflower oils and solid fats with hydrogenated cotton oil using the method of chemical transesterification.The reason is not the use of our internal raw materials, which have a lot of transisomers in the composition of hydrogenated cotton oil. In recent years, worldwide attention has been focused on the problem of transisomers of fatty acids in foods. The production of transesterified fats is a fundamentally new stage in the development of the fat processing industry, which provides a significant improvement in the quality of finished products. From the beginning, we compiled the reaction for the samples according to the corresponding ratio to № 1-initial sunflower oil, № 2 – hydrogenated cotton oil and transesterification formulations: № 3–60/40, № 4–75/25, № 5–80/20, № 6–90/10. The possibility of lowering trans acids in solid fats with the process of modifying oils and solid fats based on sodium methylate catalyst was established.

Keywords: hydrogenated cottonseed oil, trans acid, esterification, methylate sodium catalyst.

Introduction. The development of the economy of the Republic of Uzbekistan, the provision of industry with raw materials, and the population with food products. The two main areas of agriculture are farming and animal husbandry; the primary foodstuffs and raw materials necessary for human life are produced for industrial sectors. They are of particular importance for the primary or integrated processing of farmer and livestock resources and the material support of the people. Therefore, great attention was paid to the

processing of agricultural products in the first stage of economic reforms in Uzbekistan thanks to the **President Shavkat Mirziyoyev Miromonovich** [1]. The food industry is the main sector of the economy, socially protecting and supporting the population, providing with additional jobs, and also forming the budgets of small and large regions. The food industry includes many enterprises producing meat and dairy, fish, flour, bakery and confectionery, pasta, canned fruits and vegetables, tea, winemaking products and champagne, alcohol, tobacco products, beer and soft drinks, soap and especially oil and fat. The task of continuously providing the country's population with high-quality food products determines the need for the development of the food industry and as an oil and fat industry. The oil and fat industry of our Republic has rich experience and potential that allows it to occupy a leading place in the national economy. This industry is mainly focused on the processing of local raw materials [2]. Nowadays, the spread and margarine industry are very developed, but for them the raw materials are modified fats, transesterifications come from abroad [3]. The reason is not the use of our internal raw materials, which have a lot of transisomers in the composition of hydrogen oil. In recent years, worldwide attention has been focused on the problem of transisomers of fatty acids contained in food [4]. They are found in nature and are formed during hydrogenation [5]. For example, in milk and fat of ruminants, their amount does not exceed 5%, and in the process of hydrogenation it can reach 50%. Many scientists who have conducted research in this area believe that uncontrolled interference in the nature of fats can cause serious harm to human health. In many countries, the limit of such interference is defined and restrictions on the content of trans isomers in food products have been adopted at the legislative level. At present, there are two modification methods that allow one to obtain specialized fats without transisomers of fatty acids or with a low content of them: transesterification – depending on the type of catalyst, chemical and enzymatic (enzymatic) [6]. Transesterification of oils and fats is widely used in the UK, Germany, Holland, Japan, Belgium, Canada, the USA and other countries to effectively solve many problems in the production of spreads, margarines, fats for the confectionery and baking industries, including for: creating products, not containing transisomers of fatty acids; creating an optimal range of products for various purposes in terms of acid composition and rheological properties with a limited selection of raw materials [7]. The production of transesterified fats is a fundamentally new stage in the development of the fat processing industry, which provides a significant improvement in the quality of finished products [8]. The transesterification of fats and oils consists in the intra- and intermolecular redistribution of fatty acids in a mixture of triglycerides [9]. In the production of edible fats, mainly chemical intermolecular and intramolecular transesterification is used, which consists in the redistribution of fatty acid radicals under the influence of homogeneous catalysts [10]. Currently, transesterification is carried out mainly with sodium methylate or ethylate [11]. The aim of this work is to develop modified transesterifications with a reduced trans-acid content as local raw materials using liquid vegetable sunflower oils and solid fats with cotton hydrogenated oil using the method of chemical transesterification.

Objects and research method. To transesterify, we needed liquid sunflower oil with the color 5 red unit, acid number 0.2 mg KOH; brand –5 cotton hydrogenated oil, melting point 43 °C, acid number 0.4 mg KOH, hardness 360 g/cm. As a catalyst, we used sodium methylate, the indices of which are given in (Table 1).

Table 1.– The technological characteristics of the catalyst

Catalyst	Range of working concentrations,%	Operating temperature range, °C	Reaction time, min
sodium methylate	0.1–0.15	50–120	5–120

To conduct the reaction, we from the beginning compiled a sample for the samples according to the corresponding ratio to № 1 – initial sunflower oil, № 2 – hydrogenated cotton oil and transesterification formulations: № 3–60/40, № 4–75/25, № 5–80/20, No. 6–90/10. The fatty acid composition of the oil and the original hydrogenated cotton oil are given in (table 2).

Table 2. – The characteristics of the initial samples

Name of initial samples	Fatty Acid Composition											Acid number	number of saponification	Refractive Index, 25 °C	Mp °C
	14:0	16:0	16:1	17:0	18:0	18:1	18:2	20:0	20:1	22:0	24:0				
Sunflower oil	0.08	6.84	0.09	–	3.84	27.45	58.14	0.26	0.14	0.77	0.23	0.2	192	1.473	–19
Hydrogenated cotton oil	0.72	22.75	0.20	0.22	17.60	9.78	1.89	0.29	0.26	0.14	–	0.4	197	1.471	43

The transesterification process appears to be proceeding under vacuum, but for laboratory conditions, we were used under a pressure of 1 atm of nitrogen as an inert gas and to interrupt the reaction of a 25% NaCl solution [12]. For this experiment, glassware was collected; a chemical glass with a capacity of 500 cm^3; magnetic stirrer; dividing funnel per 1000 cm^3, an autoclave with a capacity of 1 l was installed, which is equipped with a nichrome spiral and nozzles for nitrogen supply, with a manometer [13]. 400 g of the mixture was weighed into a glass with an accuracy of 0.01 g, consisting of solid and liquid fats, its melting point was determined and heated to dry at a temperature of 120 °C for 0.5 h with vigorous stirring. Magnetic stirrer speed 2.0 s-1. Then, the contents of the autoclave were cooled to a transesterification temperature of 90 °C [14]. Without stopping stirring, the catalyst was added in an amount of 1% to the autoclave, in the form of a 10% oil suspension, and closing the lid, nitrogen was supplied up to 1 atm pressure, stirring was continued for a predetermined time at the same temperature [15]. The reaction mixture was placed in a separatory funnel and washed with 300 cm^3 of hot 95 °C 25% NaCl solution to destroy the catalyst, and then with hot water until neutral by methyl orange [16]. The transesterified fat was filtered through a paper filter and the melting point and hardness were determined, which is shown as a result of the discussion in (Table 4). The acid number was determined for the initial samples and the obtained transesterifications with the method for determining the acid number of light oils. This method is based on titration of a fat sample with an alkali metal hydroxide solution in the presence of a phenolphthalein indicator [17]. As a solvent for fat, a neutralized mixture of alcohol with diethyl ether or gasoline is used. **Reagents:** a neutralized mixture of 96% ethyl alcohol and diethyl ether (1: 2), 1% alcohol solution of phenolphthalein; **Chemical glassware:** flat-bottomed wide-necked flask with a capacity of 100 cm^3. **Technique of execution.** 3–5 g of fat was weighed into a flask on an analytical balance, 50 cm^3 of a neutralized mixture of diethyl ether and ethyl alcohol were poured, and the fat was dissolved. 3–5 drops of a 1% phenolphthalein solution were added to this. The resulting solution with constant stirring was titrated from the burette with a 0.1 m alcohol solution of alkali metal hydroxide until a faint pink color appeared that did not disappear for 30 s [18]. The results of acid numbers are given in (tables 2, 4).

For chromatographic data on the original sunflower oil and hydrogenated cotton oil are shown in (figures 1, 2).

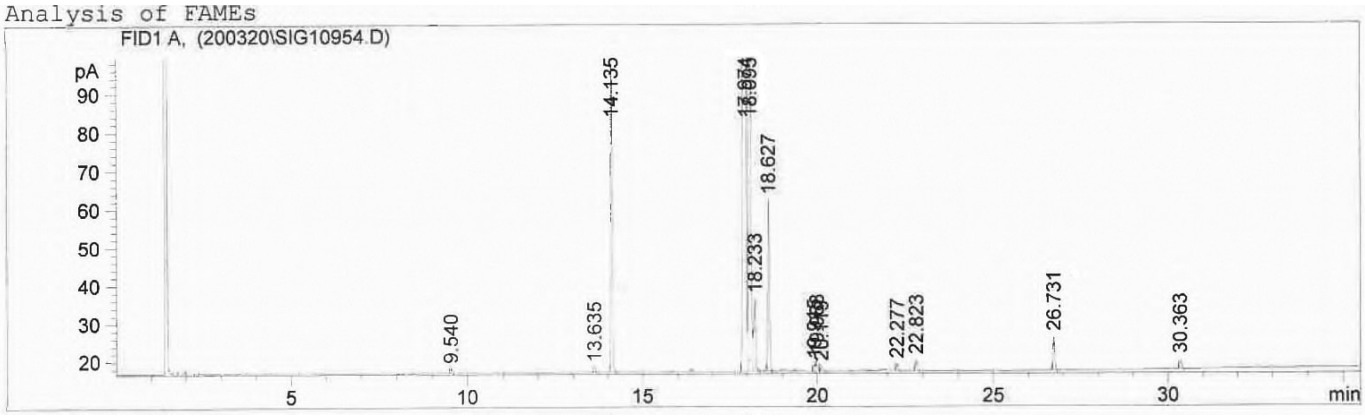

Figure 1. Chromatogram of the fatty acid composition of the original sunflower oil

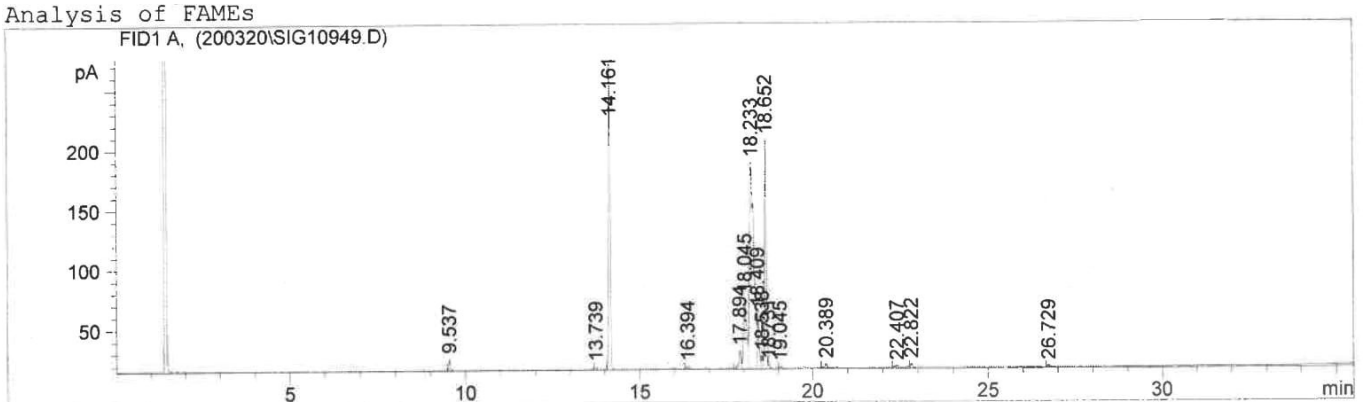

Figure 2. Chromatogram of the fatty acid composition of the starting cotton hydrogenated cotton oil

Results and discussion. Results are presented in (table 3). The obtained data on transesterification experiments are given [19]. To determine the composition of fatty acids, the presented samples, which are shown in the pictures of chromotograms 1.2 and transesterification images: No. 1–60/40, No. 2–75/25, No. 3–80/20, No. 4–90/10 were hydrolyzed with 10% methanol KOH solution in the ratio of sample: solution 1:10, while boiling in a water bath for 1 hour [20]. The resulting soaps were decomposed with a 50% aqueous solution of H_2SO_4. Fatty acids were extracted three times with diethyl ether. Next, the ether extracts were washed with distilled water to a neutral medium, dried over sodium sulfate, and then the ether was distilled off. Fatty acids were methylated with freshly prepared diazomethane. The obtained methyl esters were purified in a thin layer of silica gel in a hexane: diethyl ether 4: 1 solvent system, the ME zone was shown in J2 vapors, and methyl esters were stripped with silica gel with chloroform.

Table 3.– Fatty acid composition of the studied samples,% GC by weight

Fatty acid	Source oil	Samples				Hydrogenated cotton fat
		№ 1	№ 2	№ 3	№ 4	
1	*2*	*3*	*4*	*5*	*6*	*7*
Myristine 14:0	0.08	0.48	0.58	0.61	0.68	0.72
Palmitic 16:0	6.84	16.82	19.30	19.85	21.57	22.75
Palmitoleic 16:1	0.09	0.14	–	0.18	0.25	0.20

1	*2*	*3*	*4*	*5*	*6*	*7*
Margarine 17:0	–	0.16	–	0.20	0.20	0.22
Stearin 18:0	3.84	12.49	14.58	15.05	16.28	17.60
Oleic 18:1	27.45	16.47	13.95	13.38	11.38	9.78
Linoleic 18:2	58.14	22.79	14.68	12.56	6.78	1.89
Peanut 20:0	0.26	0.29	0.27	0.30	0.28	0.29
Eicosene 20:1	0.14	0.19	–	0.27	0.24	0.26
Begenova 22:0	0.77	0.40	0.29	0.28	0.19	0.14
Lignoceric 24:0	0.23	0.17	–	0.12	0.09	–

After chloroform removal, the MEs were dissolved in hexane and analyzed on an ***Agilent Technologies 6890 N*** instrument with a flame ionization detector using a 30 m long capillary column with an inner diameter of 0.32 mm with an deposited HP-5 phase at temperatures from 150 to 270 °C. The carrier gas is helium.The composition and content of fatty acids are presented in (table 3).

From (table 3). It can be seen that, horizontally from left to right, an increase in the concentration of solid fats increases the mass fraction of saturated fatty acids and unsaturated decreases. After washing and drying, the samples do not appear stratification of oils and fats. This is due to the intermolecular and intramolecular interchangeability of acyls (transesterification) in triglycerides in the presence of an alcoholate catalyst. Transesterification is used in industry to reduce the content of high-melting glycerides and trans isomers in fats. In (table 4) shown by lowering the transisomers from the initial hydrogenated cotton oil sequentially to recipe № 1 and as a result, the melting point of the transesterifications decreass.

Table 4.

Samples	**The content of trans isomers %**	**Saturated Fatty Acid %**	**Unsaturated fatty acid %**	**Melting point °C**	**Hardness. g/cm**	**A.n. mg KOH**
No. 1	29.60	30.81	69.19	28	80	0.2
No. 2	36.35	35.02	64.98	34	120	0.3
No. 3	37.20	36.41	63.59	36	320	0.2
No. 4	42.06	39.29	60.71	39	360	0.3
Hydrogenated cotton oil	46.37	41.5	58.5	43	500	0.4

Similar fats are obtained by transesterification of mixtures containing hydrogenated fats. Transesterified fats containing 25–35% saturated and 30–35% transmonosaturated fatty acids have a melting point of 32–33 °C, a hardness of 90–120 g / cm and are used either as ready-made greasy bases of squared margarines and cooking fats, or as their plasticizing component. Today, the margarine industry in Uzbekistan is developing on a large scale, mainly the methods of emulsion crystallization on rollers are well developed. We believe that the conclusions drawn from this experiment can be effectively applied in our similar certified products, which are produced as raw materials for margarine.

Conclusions. The possibility of lowering trans acids in solid fats with the process of modifying oils and solid fats based on sodium methylate catalyst was established. The most active transesterification catalysts include sodium methylate and ethylate. These catalysts even at relatively low temperatures

(0–130 °C) interact with mono-, di-, and triglycerides to form sodium glycerates, in the presence of even small quantities of which the transesterification reaction is sharply accelerated.

References:

1. Ukaz Prezidenta Respubliki Uzbekistan ot 07.02.2017 g. N UP-4947 "O Strategii dejstvij po dal'nejshemu razvitiju Respubliki Uzbekistan". Decree of the President of the Republic of Uzbekistan dated 07.02.2017 N UP-4947 "On the Strategy for the Further Development of the Republic of zbekistan".
2. Eychenne V., Debrauwer L., Mouloungui Z. O-etherification between glycerol and glycerol monooleate – Demonstration of formation of diglycerol monooleate and triglycerol monooleate by fast atom bombardment-mass spectroscopy and ^{13}C nuclear magnetic resonance. Journal of Surfactants and Detergents, 2000.– Vol. 2.– No. 3.– P. 173–177. Doi:10.1007/S11743-000-0122-3.
3. Rahimov D. P., Salijanova SH. D., Ruzibaev A. T., Achilova S. S., Sanaev E. SH. Determination of the optimal temperature regime during cooling and crystallization in the production of margarine for a layered pastry. Universum: himiya i biologiya, 2019.– Vol. 66.– No. 12.– P. 95–100.
4. Ivashina O. A., Tereshchuk L. V., Starovojtova K. V., Tarlyun M. A. Interesterification as an alternative way to modify transisomer free fats. Tekhnika i tekhnologiya pishchevyh proizvodstv. 2015.– T. 38.– No. 3.– P. 18–23.
5. Ruzibayev A. T., Kadirov Y. K., Rahimov D. P. Intensification of the hydrogenation process of vegetable oils with effective methods of detoxication of catalyst. European Applied Sciences, 2015.– No. 5.– P. 58–61.
6. Raquel C. R., Veronique G., Roland V., Wim D. G. Chemical and Enzymatic Interesterification of a Blend of Palm Stearin: Soybean Oil for Low trans- Margarine Formulation. Journal of the American Oil Chemists' Society. 2009.– Vol. 86.– Issue 7.– P. 681–697.
7. Tereshchuk L. V., Mamontov A. S., Starovojtova K. V. Palm Oil Fractionation Products in Spread Production. Tekhnika i tekhnologiya pishchevyh proizvodstv. 2014.– No. 3.– P. 79–83.
8. Frank D. Gunstone, vegetable oils in food technology (Composition, Properties and Uses).– USA published 2002.– 337 p.
9. Oku T. Nonoguchi M. Moriguchi T. Method of production of fatty acid alkyl esters and / or glycerine and fatty acid alkyl ester-containing composition. Patent World Organization, 2005; 021697, 2005.
10. Koritala S. Selective hydrogenation of soybean oil. III. Copper-exchanged molecular sieves and other supported catalysts. Journal of the American Oil Chemists Society, 1968; 45(3), 197–200. DOI: 10.1007/BF02915351.
11. de Luna M. D. G., Cuasay J. L., Tolosa N. C., Chung T. W. Transesterification of soybean oil using a novel heterogeneous base catalyst: synthesis and characterization of Na-pumice catalyst, optimization of transesterification conditions, studies on reaction kinetics and catalyst reusability. Fuel. 2017.– V. 209.– P. 246–253.
12. Arutyunyan N. S., Yanova L. I., Arisheva E. A., Kosachev V. S., Kamyshyan M. A. Laboratory Workshop on Fat Processing Technology. – Moscow, Agropromizdat, 1991.– 160 p.
13. Eychenne V., Debrauwer L., Mouloungui Z. O-etherification between glycerol and glycerol monooleate – Demonstration of formation of diglycerol monooleate and triglycerol monooleate by fast atom bombardment-mass spectroscopy and ^{13}C nuclear magnetic resonance. Journal of Surfactants and Detergents, 2000.– Vol. 2.– No. 3.– P. 173–177. Doi:10.1007/S11743-000-0122-3.
14. Issariyakul T., Dalai A. K. Comparative kinetics of transesterification for biodiesel production from palm oil and mustard oil. Can. J. Chem. Eng. 2012.– V. 90.– P. 342–350.

15. Ma Y., Wang Q., Sun X., Wu C., Gao Z. Kinetics studies of biodiesel production from waste cooking oil using $FeCl_3$-modified resin as heterogeneous catalyst. Renew. Energy. 2017.– V. 107.– P. 522–530.
16. Xingguo Wang., Wei Wei. Triacylglycerols fingerprint of edible vegetable oils by ultra-performance liquid chromatography-Q-ToF-MS. 18 Jun, 2019. Version 1. DOI: 10.17632/hdxtr557jc.1
17. Maynard Joslyn. Methods in Food Analysis. eBook ISBN: 9780323146814, Academic Press, 1st January 1950.– 534 p.
18. Rashid U., Anwar F. Production of biodiesel through optimized alkaline- catalyzed transesterification of rapeseed oil. Fuel. 2008.– V. 87.– P. 265–273.
19. Christopher Pohl., Nebojsa Avdalovic., Kannan Srinivasan., Satinder Ahuja.Ion Chromatography.– V. 13. Instrumentation, Techniques and Applications, 1st Edition, 9780128130766, Academic Press, 1st October, 2020.– 400 p.
20. Rakhimov D. P., Ruzibaev A. T., Tashmuratov A. N., Salijanova Sh. A. Research of the process of obtaining interesterified fat for margarine production on the basis of sunflower oil and palm stearin. Food science: Chemistry and chemistry technology journal, 2020.– Vol. 1.– No. 1.– P. 64–68.

https://doi.org/10.29013/AJT-20-3.4-10-14

Sanaev Ermat Shermatovich,
assistant
E-mail: soypro.uz@mail.ru
Rakhimov Dilshod Pulatovich,
assistant
E-mail: rahimov1984@list.ru
Baltabaev Ulugbek Narbaevich,
Doctor of technical sciences(PhD)., associate professor,
Tashkent Institute of Chemical Technology

METHODS OF FORMING PASTA AND REDUCING THE AMOUNT OF IN THE FINISHED PRODUCT WHILE IN CREASING THE EFFICTIENCY OF THE DRYING PROCESS BY FRYING IN OIL

Abstract. Many countries of the world, especially in Central Asia, produce pasta that quickly cooks and does not require preparation, and wheat flour is used as the main raw material. This delicious product is popular with consumers, but increasing the amount of fat in the product negatively affects consumer value. The aim of this study was to find out how the properties of gluten protein affect the reduction of fat in instant pasta during frying. Squeezing the thick dough gradually into a thin layer as a result of the grinding process, the pressed gluten is evenly distributed over the smooth surface of the dough, and the product is properly dried by frying in hot oil. The roasting process not only provides the product with high productivity, but also provides ease of use and delicious taste.

Keywords: instant fried noodles; Gluten; Oil content; Extrusion process rolling press process.

Introduction. The development of the economy of the Republic of Uzbekistan, the provision of industry with raw materials, and the population with food products. The two main areas of agriculture are farming and animal husbandry; the primary foodstuffs and raw materials necessary for human life are produced for industrial sectors. They are of particular importance for the primary or integrated processing of farmer and livestock resources and the material support of the people. Therefore, great attention was paid to the processing of agricultural products in the first stage of economic reforms in Uzbekistan thanks to the President Shavkat Mirziyoyev Miromonovich [1]. The food industry is the main sector of the economy, socially protecting and supporting the population, providing with additional jobs, and also forming the budgets of small and large regions. wheat, as one of the most widely consumed crops, can be converted in to a variety of processed foods such as noodles [2]. In Asian countries wheat is often eaten in the form of noodles and in western countries as pasta. Noodles are made from dough of wheat flour mixed with water during which the conjugation of gliadin and gluten, as the main components of wheat protein, forms gluten network structure.The formation of gluten network influences dough properties such as elasticity and viscosity [3; 4]. In noodles, the gluten network affects the viscoelasticity of the dough and determines the quality of the endproduct [5; 6]. In conventional methods for producing fried noodles, the noodle sheet is made from dough using a rolling –press followed by repeated compressions to gradually reduce the thinckness to obtain the final rolled

noodle sheet with a dense and well dispersed gluten network. Thus, wheat gluten plays an important role in processing these types of food.instand noodles have been spreading world wide. deep frying is performed in a very short time to provide hygienicand long life product at a low coast. They can be eaten shortly aafter adding hot water, and have the desirable roast and savory flavors formed during frying [7; 8]. These flavors are popular with consumers but the product is rich in oil with a high calorie content Recently, especially in developed countries excessive energy intake has been a health concern [9].

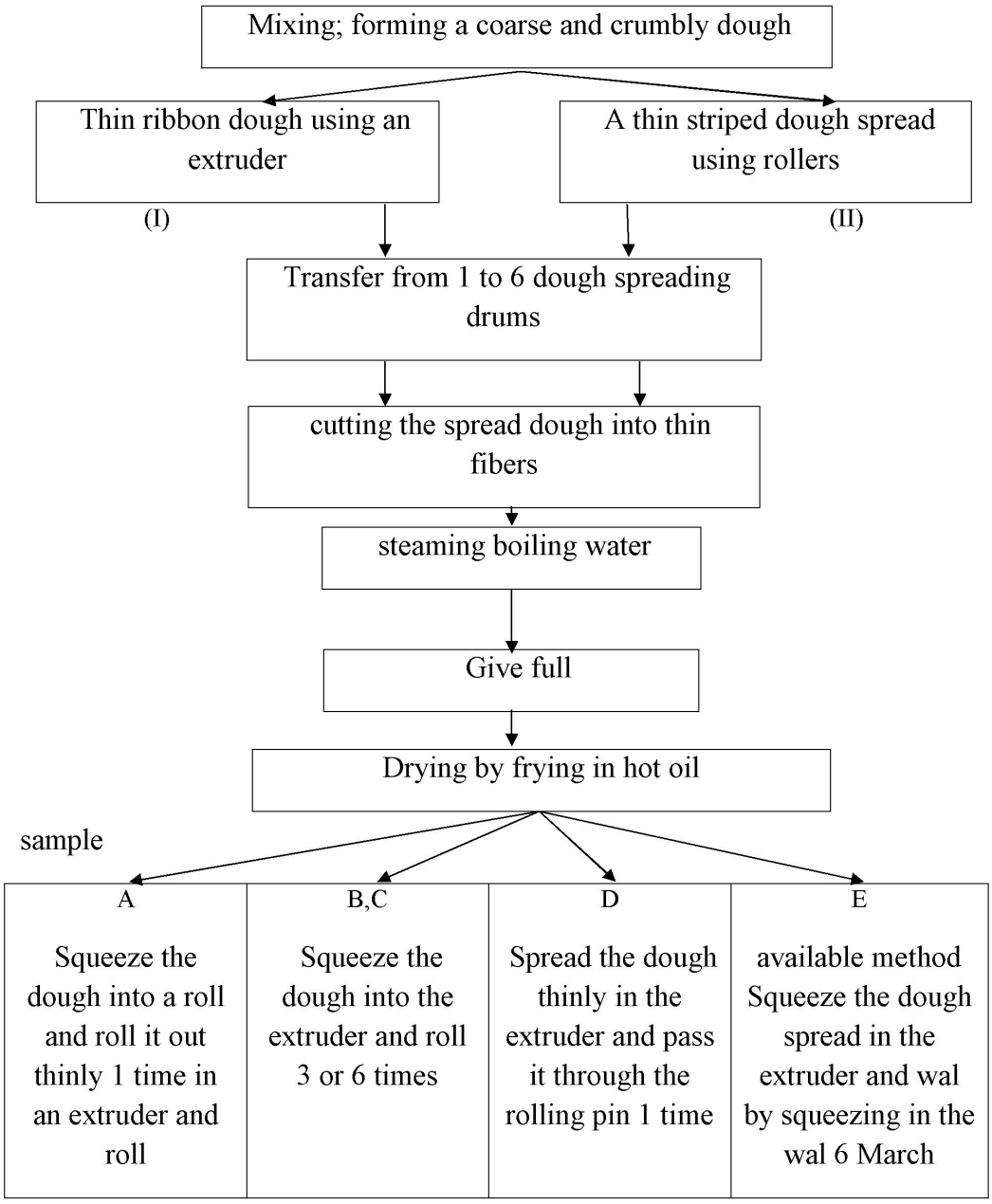

Figure 1. Schematic representation of sample preparati

As the consuotion of instant noodles has increased, areduction in the amout af oil in fried noodles is required occasionally.Several studies on the oil content of fried noodles have been reported. When whole grain flour was used, the oil content of the fried noodles decreased by up to 30% compared with this made from white flour [10]. The wet cultivar also affected the oil content has been found to in crased [11]. Thus as the noodle goes through these process the quality of the end product is product is affected by many factors however no report has yet directly investigated the relationship between the structure of the dough gluten network and the oil content of the fried noodle.this study aims to reveal how the oil content of fried noodles is affected by the formation of the gluten network during their production in particular, we will investigate how the formation of the noodle sheets and the rolling press producing affects the density of the gluten network and the oil content of the fried noodle.overall we propose a new method by changing the formation and the rolling press processes for producing noodle sheet Although some repots on regulating the oil content of instant noodles are available [12]. our method aims to improve the control of the oil content of the control of the oil content of fried noodles produced an industrial scale.

Materials and methods

The preparation of samples is shown as a flow sheet in (figure 1). Procedure E is a standard procedure. **Materials:** The ingridients used in this study were an all purpose semi strong wheat flour (protein content 10%ash content 0.38 moisture content 14.0%)tapioca starch ash content 0.33% moisture content 13.6% dietary sodium chloride polyphosphate main component sodium polyphosphate kansui main ingredients sodium carbonate and potassium carbonate monosodium glutamate soy sauce and meat extract.all ingridients were commercially purchased.

Table 1.– Characterization of fried-noodles made by different procedures

Sample	Sheet making	Storci Pres	Oil conten (%)	Cross-section alarea(um^2)×10^5	Total void area (um^2)×10^5	Void number	Void Radio (%)
A	**Extruder**	1	10.4	1.2	1.52	14	10.8
B	**Extruder**	3	13.6	1.54	2.70	353	16.0
C	**Extruder**	6	12.5	1.75	3.26	351	18.3
D	**Storci pres**	1	11.0	1.55	2.21	275	14.5
E	**Storci pres**	6	15.2	1.9	6.07	62	27.8

Noodle preparation

***Mixing*: A** slurry was prepared by dissolving dietary sodium chloride 12 g kansui 1.8 g and polymeric to a total volume of 350 ml.Coarse and crumbly dough was prepared by adding the slurry to a mixture of semi strong wheat flour 800g 200g

Noodle sheet formation

Preparation of extrude.d noodle sheets: Noodle sheets 7 mm thick were prepared using a noodle extruder the prepared dough was extruded through a rectangular hole 225 × 7mm at feed rate of 350g/min these products are referred to as extruded noodle sheets.

Preparation of compound rolled noodle sheets: coarse noodle sheets were prepared using a forming roller from the some dough as prepared above. Pairs of coarse noodle sheets were pressed together using a compound roller to create a 7.0 mm thick noodle sheet. these products are referred to us rolled noodle sheets. **Storci –press** the noodle sheets were rolled between 1 and 6 times, yielding with a final thickness of 1mm.

Extruded noodle sheets: three treatments of extruded noodle sheets(A, B and C)were prepared differing of number of times they were rolled 1–6 times. **A** Extruded noodle sheets were rolled

once compressing them from thickness of 7.0 mm to 0.8;

B: Extruded noodle sheets were rolled 3 times compressing them stepwise from a thickness of 8.0 mm to 2.0 mm 1.0 mm and the to 1.5 mm;

C: Extruded noodle sheets were rolled 6 times compressing them stepwise from a thickness of 8.0 mm to 4.0 mm to 3.0 mm to 2.5 mm to 2.2 mm to 1.5 mm and the to 1.0 mm.

Rolled noodle sheets: two treatments of rolled noodle sheets D and E were prepared, differing in the number of times they were rolled (1–6) times;

D: Rolled noodle sheets were rolled 6 times compressing them them from a thickness of 8.0 mm to 1.0;

E: Rolled noodle sheets were rolled once compressing them from a thickness of 8.0 mm to 4.0 mm to 3.0 mm to 2.5 mm to 2.0mm to 1.5 mm and then to 1.0 mm **cutting** all noodle sheets were compressed to 1.0 mm;

B: Extruded noodle sheets were rolled 3 times compressing them stepwise from a thickness of 8.0 mm To 2.0mm to 1.5 mm and then to 1.0;

C: extruded noodle sheets were rolled 6 times compressing them stepwise from a thickness of 8.0mm to 4.0 mm to 3.0 mm to 2.5 mm to 2.0 mm to 1.5 mm and then to 1.0 mm;

E: rolled noodle sheets were rolled 6 times compressing them stepwise from a thickness of 8.0 mm to 4.0 mm to 3.0 mm to 2.5 mm to 2.0 mm to 1.1 mm;

Cutting: All noodle sheets were compressed to 1.0 mm in thickness by rolling press then cut into strings using a square noodle cutter 1.5 mm pitch these products are referred to as raw cut noodle strings.

Steam treatment: The raw cut noodle strings were immersed for 5 seconds. In a flavoring solution (60 °) containing dietary sodium chloride (80g/l) monosodium glutamate (13.5 g/l) soy sauce 10ml/l and meat extract 30g/l.

Deep frying and drying after the flavoring treatment the noodle strings were dried by deep frying them in palm oil for 145 seconds at around (150 °C) to evaporate the water giving a final water content of approximately 2.0%.

Conclusion

This study confirmed that dough from traditional fried instant pasta is coarse. After examining the relationship between gluten protein content and the structure of dough for instant pasta, it was found that less fat is left in the gluten net when frying dough for pasta, which is thin-coated. It is also possible to combine extruded pastes with a thin layer, minimizing the thickness of the dough. As a specific method, it may be proposed to standardize the number of movements of the spreading presses, to ensure the formation of gluten protein, and to help reduce the calorific value of instant pasta.

References:

1. Ukaz Prezidenta Respubliki Uzbekistan ot 07.02.2017 g. N UP-4947 "O Strategii dejstvij po dal'nejshemu razvitiju Respubliki Uzbekistan". Decree of the President of the Republic of Uzbekistan dated 07.02.2017 N UP-4947. "On the Strategy for the Further Development of the Republic of zbekistan".
2. Eychenne V., Debrauwer L., Mouloungui Z. O-etherification between glycerol and glycerol monooleate – Demonstration of formation of diglycerol monooleate and triglycerol monooleate by fast atom bombardment-mass spectroscopy and ^{13}C nuclear magnetic resonance. Journal of Surfactants and Detergents, 2000.– Vol. 2.– No. 3.– P. 173–177. Doi:10.1007/S11743-000-0122-3.
3. Rahimov D. P., Salijanova SH. D., Ruzibaev A. T., Achilova S. S., Sanaev E. SH. Opredelenie optimal'nogo temperaturnogo rezhima pri ohlazhdeniii kristallizacii v proizvodstve margarina dlya sloenogotesta (Determination of the optimal temperature regime during cooling and crystallization in the production of margarine for a layered pastry). Universum: himiya i biologiya, 2019.– Vol. 66.– No. 12.– P. 95–100.

4. Ivashina O. A., Tereshchuk L. V., Starovojtova K. V., Tarlyun M. A. Pereeterifikaciya kak al'ternativnyj sposob modifikacii zhirov, svobodnyh ot transizomerov Interesterification as an alternative way to modify transisomer free fats. Tekhnika i tekhnologiya pishchevyh proizvodstv. 2015.– T. 38.– No. 3.– P. 18–23.
5. Matsunaga A., Kainuma K. Studies on the retrogradation of starch in starchy foods. Part 3. Effect of the addition of sucrose fatty acid ester on the retrogradation of corn starch. Starch Stärke 38: 1986.– P. 1–6.
6. Deng Z., Tian J., Zhao L., Zhang Y., Sun C. High temperature-induced changes in high molecular weight glutenin subunits of Chinese winter wheat and its influences on the texture of Chinese noodles. J Agron Crop Sci 194: 2008.– P. 262–269.
7. Kaur A., Singh N., Kaur S., Katyal M., Virdi A. S., et al. Relationship of various flour properties with noodle making characteristics among durum wheat varieties. Food Chem 188: 2016.– P. 517–526.
8. Katagiri M., Kitabatake N. Rheological properties of somen noodles-A traditional Japanese wheat product. J Food Sci 75: 2010. E51–E58.
9. Niu M., Hou G. G., Wang L., Chen Z. X. Effects of superfine grinding on the quality characteristics of whole-wheat flour and its raw noodle product. J Cereal Sci 60: 2014.– P. 382–388.
10. Li M., Zhu K. X., Wang B. W., Guo X. N., Peng W. et al. Evaluation the quality characteristics of wheat flour and shelf-life of fresh noodles as affected by ozone treatment. Food Chem 135: 2012.– P. 2163–2169.
11. Silva E., Sagis L. M.C., Van der Linden E., Scholten E. Effect of matrix and particle type on rheological, textural and structural properties of broccoli pasta and noodles. J Food Eng 119: 2013.– P. 94–103.
12. Patel M. J., Chakrabarti-Bell S. Flour quality and dough elasticity: Dough sheetability. J Food Eng 115: 2013.– P. 371–383.

https://doi.org/10.29013/AJT-20-3.4-15-22

Ergashev N. A.,
Senior teacher
Isomidinov A. S.,
Senior teacher,
"Ferghana polytechnic institute" Republic of Uzbekistan
E-mail: Isomiddinov1985@mail.ru
Alimatov B. A.,
doctor of technical sciences, professor
"Belgorod State University of Technology
named after B. G. Shukhov" Russian Federation

DETERMINATION HYDRAULIC RESISTANCE OF DEVICE THAT HAS THE VORTEX FLOW CREATING CONTACT ELEMENT

Abctract. In the article, results of experiments which were carried out in wet dusty gas cleaning device for determination of total hydraulic resistance are given. For experiment's results processing scheme was designed. In experimental device hydraulic resistance that influences to the dusty gas velocity and the liquid. On basics of experiments local resistance coefficient in metallic tube and resistance coefficient in contact element were determined.

For experimenting different parameters were selected: hole in the filter material has different diameters d_f= 2; 2, 5; 3 mm; velocity of gas in the apparatus v_z = 7.07 ÷ 28.37 m/s (The velocity range is close to the speed range imposed on dust-cleaning devices in industry-wide wet methods); The experiments were conducted in air and water systems at a temperature of 20 ± 2 °C.

Keywords: wet method, vortex flow creating element, dusty gas, surface tension, toxic gas, air flow, gas flow, gas velocity.

Introduction

One of the main features of the design is the improvement of design schemes based on the selection of the optimal values of resistance of the working bodies of the device to the dust gas flow in the wet gas treatment facilities.This characteristic determines the hydraulic resistance of the device and the permissible amount of working fluid leaving the unit with gas [1; 3; 4]. In addition, increased hydraulic resistance in the working body of the unit can improve the efficiency of cleaning, but also result in reduced performance and compression of dust particles into pipes. This in turn increases energy consumption.

Numerous research works have been carried out to determine the optimal values of these factors [5; 6; 7 and others]. However, a complete solution for achieving maximum cleaning efficiency and maximizing performance at minimum hydraulic resistance values has not been developed.

A general study of these problems has been made, a wet gas purification device with a contact coil [2] has been developed, and a three-step research to determine the effect of hydraulic resistance and purification efficiency and energy consumption. In (figure 1), an overview of the experimental device is given.

Research object and method

Pressure loss is observed in the working bodies of wet gas cleaning devices. This is explained by the structure of the device and the number of working bodies.

The contact element consists of a metal pipe 3 that directs the flow of the gas and a contact element 15 with a rotating spin on the gas flow. This condition is called loss of pressure in working bodies.

Then the total hydraulic resistance of the device can be written as follows, Pa;

$$\Delta P = P_1 + P_2, \quad (1)$$

where: $\varnothing P$ – total hydrolic resistance of device, Pa; P_1 – hydrolic resistance in dictance between insurge flow of gas to the device and by the vortex flow creation contact element, Pa; P_2 – hydrolic resistance that in the vortex flow creating tool of device, Pa.

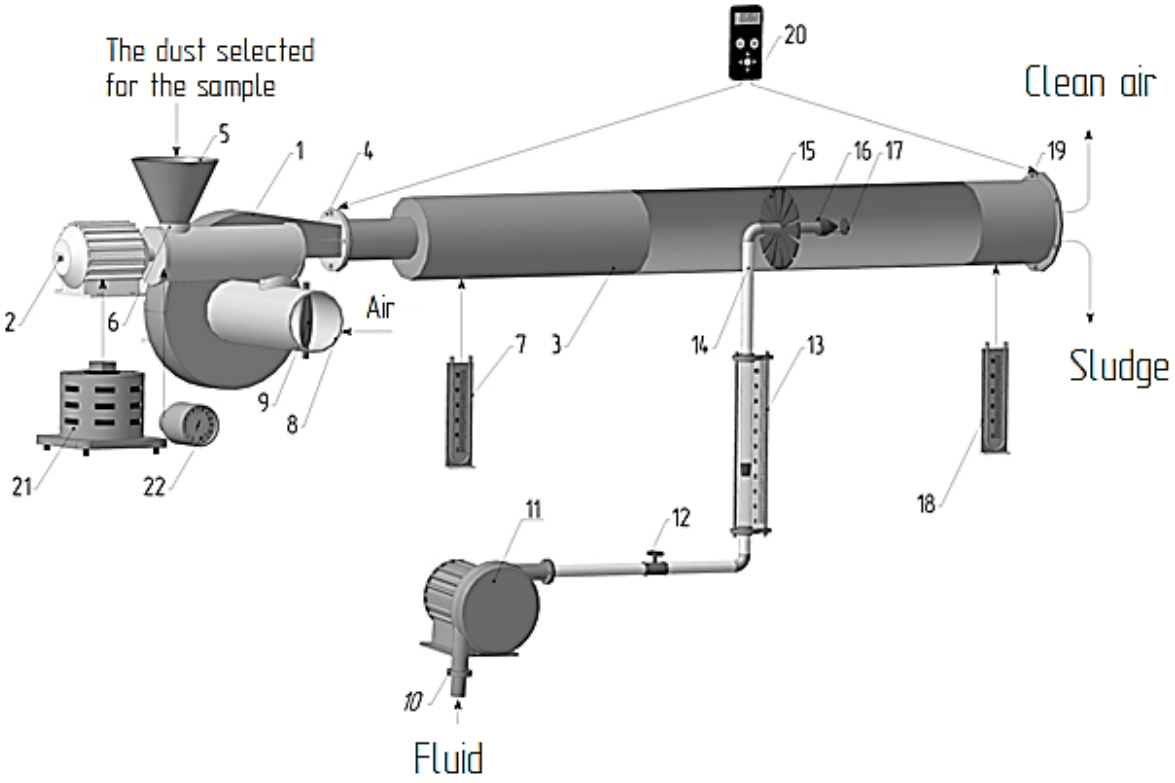

Figure 1. Total view of experimental device:

1 – fun; 2 – electromotor; 3 – metallic tube; 4, 10, 19 – flange; 5 – dust loading device; 6 – feeding uni; 7, 18 – Prandtl tube; 8 – insurge nipple of dusty gas; 9 – shiber; 11 – pump; 12 – tap; 13 – rotameter; 14 – water supplying tube; 15 – vortex flow creating contact element; (swirler) 16 – water spraying nipple; 17 – water entrainment trap; 20 – anemometer; 21 – latr; 22 – tachometer

For the determination of hydraulic resistance in working bodies, the Darcy-Weissbach equation is used, Pa [8].

$$\Delta P = \xi \frac{\rho_г \cdot \upsilon_г^2}{2} \quad (2)$$

where ρ_g – gas density, kg/m^3; v_g – lost gas velocity in working bodies of device, m/sec; ξ – hydraulic resistance which impacts to the gas flow in working bodies.

Determination and calculation of resistance coefficients are complex and require different deviations, which can only be found by experiment.

It has been studied that the total resistance coefficient of a contact element bending current depends on the above factors. In this case, it is possible to write the equation of determining the total resistance coefficient of the working body on the dusty gas flow in the unit.

$$\xi_{gen} = \xi_1 + \xi_2, \quad (3)$$

where ξ_1 – the local resistance coefficient of the dust gas to the inlet device and the contact element forming the heater is determined by the following equation;

$$\xi_1 = \lambda \frac{l}{d_e} \quad (4)$$

where l – tube length, m; d_e – equivalent diameter of tube, m; λ – The coefficient of the Darcy is that it depends on many factors in expressing the law of change with the empirical equations. Based on the structure of the experimental apparatus, the definition of the Darcie coefficient in the equation by Blazius's law was introduced [8]. Then equation (4) will look as follows;

$$\xi_1 = \frac{0.3164 \vartheta_g^2 l}{d_g \sqrt[4]{\mathrm{Re}}} \quad (5)$$

Results of experiments

In the first phase of the study, the local resistance coefficients and the values of the change factors in the distance to the inlet device and the contact element forming the heater based on equation (5) were determined experimentally. The values of the resistance coefficients and the variables are presented in (Table 1).

Table 1.– Dependence of the local resistance coefficient on the contact factor with the changing factors

v_g, m/s	7.07	15.45	22.48	24.32	28.37
Re	$5 \cdot 10^4$	$1.2 \cdot 10^5$	$1.6 \cdot 10^5$	$1.8 \cdot 10^5$	$2 \cdot 10^5$
l, mm	1000	1000	1000	1000	1000
d_e, mm	100	100	100	100	100
ξ_1	0.7	0.62	0.65	0.7	0.7

As can be seen from the values in (Table 1), the local resistance coefficients in the metal pipe are close to each other at different values of the variables. Then the coefficient of local resistance is assumed to be 0,7 with sufficient accuracy and average.

ξ_2 – the resistance coefficient of the contact element that forms the heap. Determination and calculation of resistance coefficients are complex and require different deviations, which can only be found by experiment. In this case, the following equation was obtained and the correction coefficient was used to determine the ratio of the total surface of the contact element shields to the flow-through area. The contact element is shown in (Figure 2).

$$\xi_2 = \Delta k \frac{4\pi R^2}{nab \sin\beta}, \quad (6)$$

where n – number of impellers; a, b – length of impeller's butt; β – surface's angle of slope; Δk – correlation coefficient.

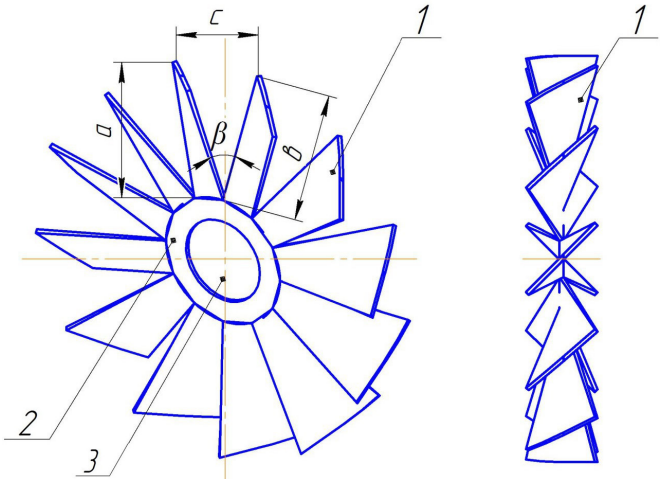

Figure 2. Total view of contact element

1 – impeller; 2 – cycle; 3 – stiffening hole

The resistance coefficient values for the contact element were calculated experimentally based on equation (6) for different values of the variables. In angle of slople for gas passage surface is sin $\beta = 60^{o}$ contact element has resistance coefficient $\xi_2 = 1.1$ and angle of slope for gas passage surface is sin$\beta = 45^{o}$ contact element has resistance coefficient $\xi_2 = 1.3$ and correlation coefficient $\Delta k = 0.91$. And last but not least angle of slope for gas passage surface is sin$\beta = 30^{o}$ contact element has resistance coefficient $\xi_2 = 1.5$ and correlation coefficient $\Delta k = 0.68$.

In angle of slope is sin$\beta = 60^{o}$ the total resistance of the device is $\xi_{gen} = 1.8$; in sin$\beta = 45^{o}$ total resistance coefficient is $\xi_{gen} = 2$ and in sin$\beta = 30^{o}$ total resistance coefficient is $\xi_{gen} = 2.2$ are proved experimentally. Figure 3–4 illustrates the correlation coefficient of correction of the resistance coefficient and the slope of the slope of the surface of the gas with the resistance coefficient.

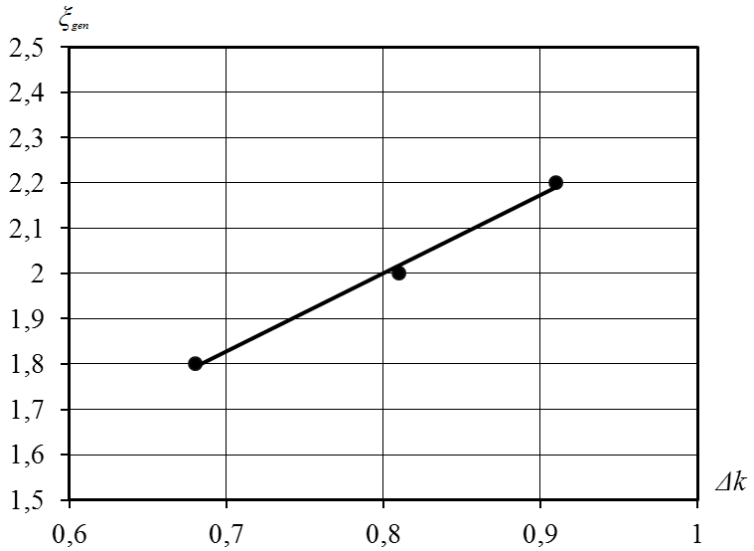

Figure 3. Dependence of total resistance coefficient with the correlation coefficient

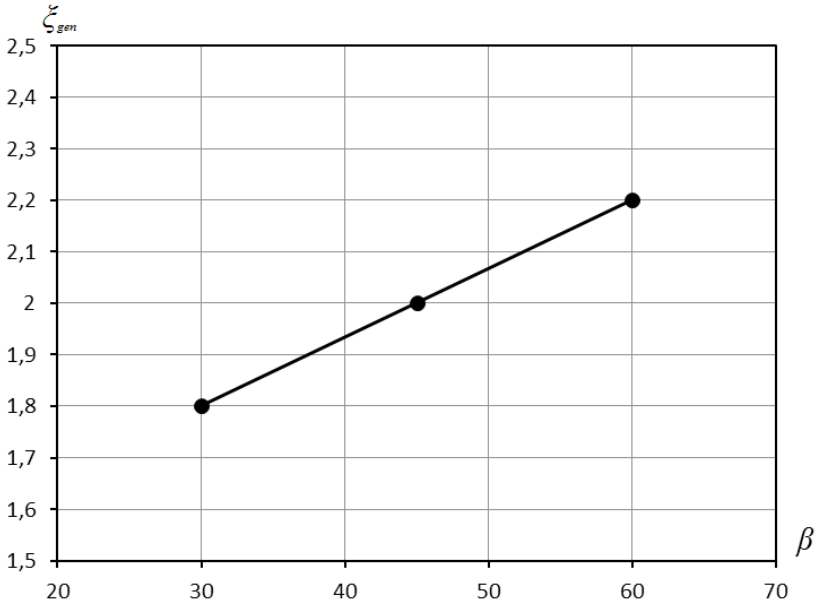

Figure 4. Dependence of total resistance coefficient ξ_{gen} with gas passage surface's angle of slope

Graphs 3, 4 are obtained through the method [10] and determined folowing formulas;

1) Dependence of the total resistance coefficient ξ_{gen} to the correlation coefficient Δk

$$y = 1.7293x + 0.6165 R^2 = 0.9944, \quad (7)$$

2) On the dependence of the total resistance coefficient ξ_{gen} to the slope of the surface of the gas by the flow of raw gas.

$$y = 0.0133x + 1.4\ R^2 = 0.9978. \quad (8)$$

Using the experimental values obtained in the second step, the hydraulic resistance of the given device was not fluid, and the hydraulic resistance of the given device was experimentally determined.

Hydraulic resistance of a non-liquid device vortex flow creating element's angles of slope α = 30 °; 45 ° and 60 °; number of impllers which gives movement to the gas n = 12; air density 1.29 kg/m^3, gas velocity v_z = 7.07 ÷ 28.37 m/s with step is increased 4 m/s; experiments had been carried out in 20 ± 2 °C temperatures.

Experiments results are given on (figure 5).

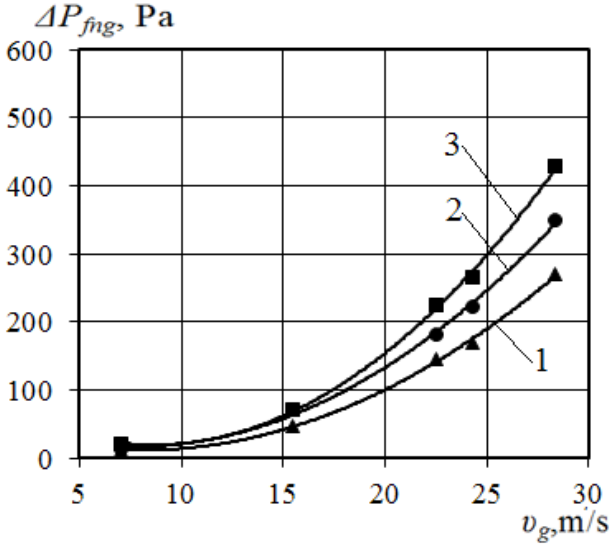

Figure 5. Dependance of gas velocity changes on hydrolic resistance ΔP_c in without liquid supplying apparatus

Figure 5 shows that if operating part of contact elemen has the folowing angles 30 °; 45 ° and 60 ° hydraulic resistances were changed from 12Pa by 21.2 Pa and in high diapazone of gas velocity hydraulic resistances were had the 270 Pa to 470 Pa changes.

At a small value of the gas velocity supplied to the unit, the flow is sparse and the pressure loss in the unit is close to each other, as the gas velocity increases, the flow is compacted and the hydraulic resistance increases.

The following empirical formulas, obtained by the least squares method of the graph dependencies presented in (Figure 5) [10], are obtained;

Dependence of gas velocity v g on hydraulic device on DPs on hydraulic resistance;

1) $y = 0.6176x^2 - 9.8756x + 51.272$; $R^2 = 0.99897$, (9)

2) $y = 0.7627x^2 - 11.63x + 60.998$; $R^2 = 0.998$, (10)

3) $y = 1.0398x^2 - 17.921x + 97.084$; $R^2 = 0.9983$. (11)

The working fluid leaking from the circuit breaker 16 on the device is hit by a retractable barrier 17 and spreads evenly across the wall of the unit. The flattening of the working fluid along the wall of the device provides a contact element with a rotating flow of dust and gas entering the unit through the ventilator 1, and a sliding fluid film is formed on the inner walls of the unit. Dust gas is hit at the corner of the blanket film formed on the wall of the device and is in contact with the working fluid and the working liquid retains dust particles. The purified gas is released into the atmosphere. The

resulting sludge flows from the device to the sludge stack through the trunk.

The thicker the film layer, the better the cleaning efficiency. But hydraulic resistance causes an increase. In addition, the film thickness causes an increase in the amount of liquid leaking out of the device with the purified gas. The boundary of the film is linear. Investigating the film layer is a complex process, which usually takes into account the hydraulic resistance of the device and the amount of fluid consumed in the study of the dependence of the treatment efficiency on the film thickness [9]. As the film thickness was not the main purpose of the research work, the hydraulic resistance of the given device was investigated depending on the amount of fluid consumed.

In the third step, the hydraulic resistance of the fluid-injected device was experimentally determined. The study was conducted in various parameters and within the following limits: The slope of the unit with a slope of contact elements moving inward to the gas flow α = 30 °, 45 ° and 60 °; number of shovels perpendicular to the contact element gas flow n = 12; The diameter of the liquid-dispersing strainer hole is d_{sh} = 2; 2,5 and 3 mm; fluid consumption Q_{liq} = = 0.07 ÷ 0.327 m³ / h (in experiments the intermediate step was increased by 0.044 m³ / h); gas density ρ = 1.29 kg / m³; gas velocity v_g = 7.07 ÷ 28.37m/s (experimentally increased with 4 m/s); the external temperature was chosen 20 ± 20 ° C for the gas and water system.

Comparative graphs for low and high hydraulic loads are constructed considering the multivariate experiments. The results of the experiments are presented in (Figures 6; 7 and 8).

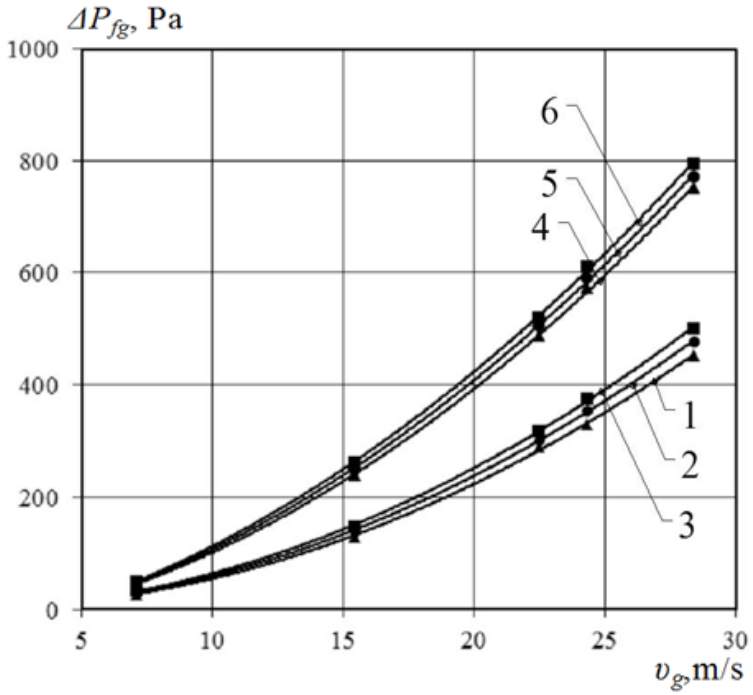

Figure 6. dependance of gas velocity v_r on hydrolic resistance ΔP_c in the liquid spraying apparatus, α = 60 °– const

n 1 – d_{sh}= 2 mm Q_{liq}= 0.07m³/h; in 2–d_{sh} = 2.5 mm Q_{liq} = 0.071 m³/h; in 3–d_{sh} = 3 mm Q_{liq} = 0.072 m³/h; in 4–d_{sh} = 2 mm Q_{liq} = 0.253 m³/h; in 5–d_{sh} = 2.5 mm Q_{liq} = 0.295 m³/h; in 6–d_{sh} = 3 mm Q_{liq} = 0.327 m³/h;

Figures 6, 7 and 8 showes that when gas velocity is v_g = 7.07 ÷ 28.37 m/s interval with the step 4 m/s and angles of slope of contact element α = 30 °;45 ° and 60 ° are increased hydraulic resistance had least loading. For the minimal liquid flowrate d_{sh} =2 mm. Q_{liq} = 0.07 m³/h–const for ΔP_{fg} = 27.4 ÷ ÷ 627.5 Pa, d_{sh} =2.5 mm. Q_{liq} = 0.071 m³/h –const for ΔP_{fg} = 29.8 ÷ 658.9 Pa.

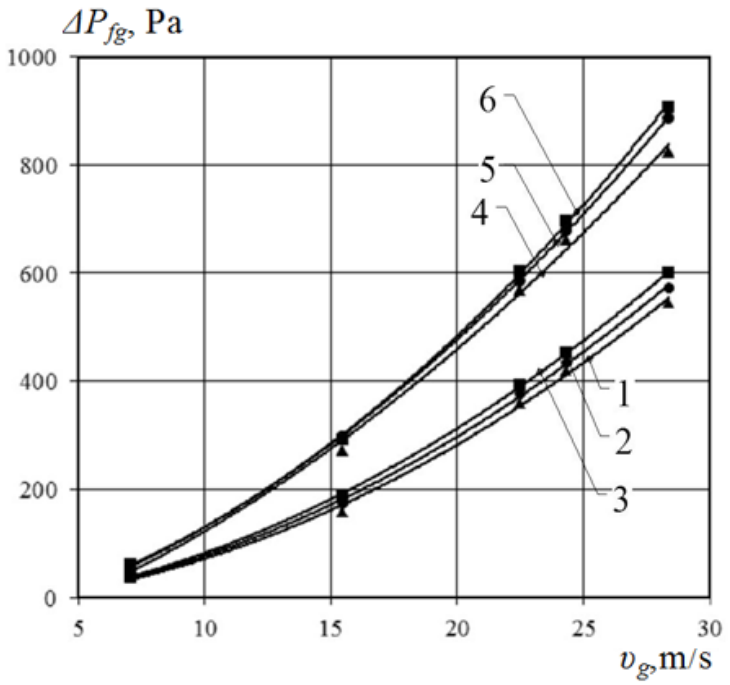

Figure 7. Dependance of gas velocity υ_r on hydrolic resistance ΔP_c in the liquid spraying apparatus, α = 450 – const

In 1 – d_{sh} = 2 mm Q_{liq} = 0.07 m^3/h; in 2 – d_{sh} = 2.5 mm Q_{liq} = 0.071 m^3/h; 3 – d_{sh} = 3 mm Q_{liq} = 0.072 m^3/h; in 4 –d_{sh} = 2 mm Q_{liq} = 0.253 m^3/h; in 5 – d_{sh} = 2.5 mm Q_{liq} = 0.295 m^3/h; in 6 – d_{sh} = 3 mm Q_{liq} = 0.327 m^3/h;

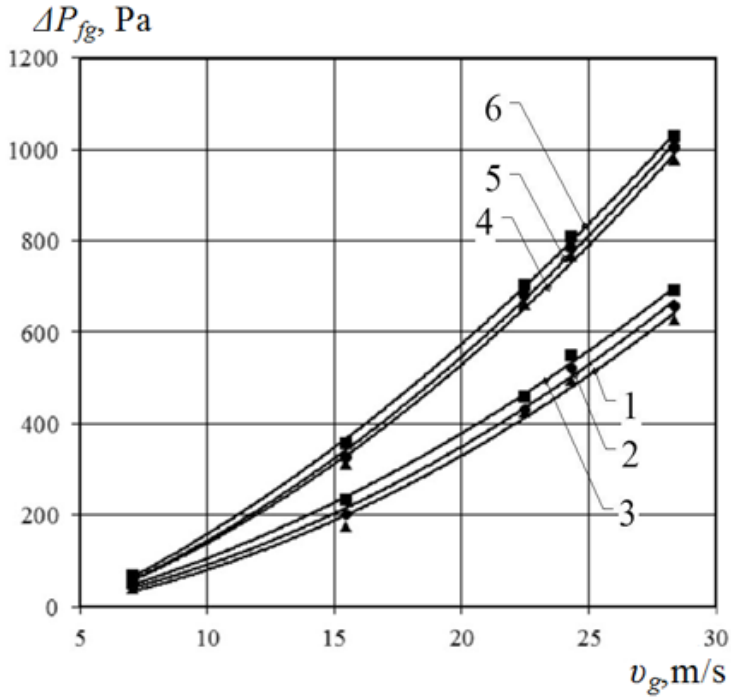

Figure 8. Dependance of gas velocity υ_r on hydrolic resistance ΔP_c in the liquid spraying apparatus, α = 30 °– const

In 1 – d_{sh} = 2 mm Q_{liq} = 0.07 m^3/h; in 2 – d_{sh} = 2.5 mm Q_{liq} = 0.071 m^3/h; in 3 – d_{sh} = 3 mm Q_{liq} = 0.072 m^3/h; in 4 – d_{sh} = 2 mm Q_{liq} = 0.253 m^3/h; in 5 – d_{sh} = 2.5 mm Q_{liq} = 0.295 m^3/h; in 6 – d_{sh} = 3 mm Q_{liq} = 0.327 m^3/h;

High hydraulic resistance for maximum fluid consumption $d_{ш}$ = 2 mm. Q_{liq} = 0.253 m^3/h –const for ΔP_{fg} = 45.9 ÷ 978.5 Pa, d_{sh} = 2.5 mm. Q_{liq} = 0.295 m^3/h – –const for ΔP_{fg} = 47.8 ÷ 1003.2 Pa and d_{sh} = 3 mm. Q_{liq} = 0.327 m^3/h–const for ΔP_{fg} = 49.8 ÷ 1028.3 Pa.

The following empirical formulas were obtained using the least squares method of graphical dependencies presented in (Figures 6; 7 and 8).

Depending on the hydraulic resistance of the working body of contact elements moving in a gas flow v_g and angle of slope contact element;

α = 60 ° – const

1) $y = 0.5754x^2 – 0.3434x + 0.5387$; $R^2 = 0.9996$ (12)
2) $y = 0.5892 \times 2 + 0.2554x – 2.3743$; $R^2 = 0.9998$ (13)
3) $y = 0.6089 \times 2 + 0.5873x – 3.0193$; $R^2 = 0.9997$ (14)
4) $y = 0.7587x^2 + 6.4326x – 38.56$; $R^2 = 0.9998$ (15)
5) $y = 0.733x^2 + 9.1652x – 52.343$; $R^2 = 0.9998$ (16)
6) $y = 0.733x^2 + 9.1652x – 52.343$; $R^2 = 0.9998$ (17)

α = 45 ° – const

1) $y = 0.6158x2 + 2.6351x – 16.762$; $R^2 = 0.9983$ (18)
2) $y = 0.6248 \times 2 + 3.3384x – 19.484$; $R^2 = 0.9992$ (19)
3) $y = 0.629 \times 2 + 4.2042x – 23.17$; $R^2 = 0.9997$ (20)
4) $y = 0.6242 \times 2 + 15.003x – 90.469$; $R^2 = 0.9978$ (21)
5) $y = 0.7804 \times 2 + 11.375x – 62.745$; $R^2 = 0.9984$ (22)
6) $y = 0.8771 \times 2 + 9.0507x – 48.405$; $R^2 = 0.9996$ (23)

α = 30 ° – const

1) $y = 0.5754 \times 2 – 0.3434x + 0.5387$; $R^2 = 0.9996$ (24)
2) $y = 0.5892 \times 2 + 0.2554x – 2.3743$; $R^2 = 0.9998$ (25)
3) $y = 0.6089 \times 2 + 0.5873x – 3.0193$; $R^2 = 0.9997$ (26)
4) $y = 0.7587 \times 2 + 6.4326x – 38.56$; $R^2 = 0.9998$ (27)
5) $y = 0.7401 \times 2 + 7.9696x – 46.473$; $R^2 = 0.9998$ (28)
6) $y = 0.733 \times 2 + 9.1652x – 52.343$; $R^2 = 0.9998$ (29)

Conclusion

From the three-stage experiments on hydraulic resistance, we can conclude that increased fluid intake strengthens the liquid film on the inner surface of the pipe. This in turn increases the hydraulic resistance. In addition, the increase in gas velocity supplied to the unit significantly influences hydraulic resistance. Increased hydraulic resistance improves cleaning efficiency but increases energy costs for dust gas cleaning. Therefore, achieving high purification efficiency at minimum hydraulic resistance values is an important issue.

References:

1. Valdberg A. Y., Nikolaykina N. Y. Processes and devices for environmental protection.– Moscow: "Drofa", 2008.– 239 p.
2. Alimatov B. A., Ergashev N. A., Karimov I. T. "Wet dust cleaning device that has the vortex flow creating contact element", FarPI, Journal of Science and Technology,– Issue 2, 2019 year.– P. 149–152.
3. Usmanova R. R. Improving the efficiency of gas purification in inertial apparatus with active hydrodynamics Diss.d.t.n. UFA-2017.– 171 p.
4. Aliyev G. M. Dust collection and purification technology for industrial gases.– Moscow: Metallurgy, 1986.– 544 p.
5. Patent: RF2403951. B01D47 / 06 Usmanova R. R., Panov A. K. "Bubble-exhaust device with a conical swirl": 11/20/2010. Bleu.– Number 32.
6. Patent: RF2316383. B01D47/06 Zhernakov V. S., Usmanova R. R., Panov A. K. "Bubbling-exhaust device with axial irrigation" 02/10/2008. Bleu.– Number 4.
7. Patent: RF21823843. B01D47 / 06 Panov A. A., Titov V. M., "Bubble-vortex apparatus" 05.27.2002.
8. Latipov K. Sh. "Hydraulics and hydro machine".– Tashkent, Uktuvchi, 1992 y.– P. 75–80.
9. Isomiddinov A. S. The study of the hydraulic resistance of the rotor-filtering apparatus // Scientific journal of technical sciences Universum.– Moscow, 2019.– No. 10(67).– P. 54–58.
10. Vygodsky M. Ya. Handbook of higher mathematics // – M.: Nauka, 1972.– 872 p.

Section 2. Chemistry

https://doi.org/10.29013/AJT-20-3.4-23-31

Abdurazakov Asqar,
Ph.D in Chemistry., Senior researcher,
Institute of chemistry of plant substances Academy
of sciences of the Republic of Uzbekistan, Republic of Uzbekistan, Tashkent
E-mail: asqar2606@mail.ru

Khvan Alla,
Ph.D. in Chemistry., Senior researcher,
Institute of chemistry of plant substances Academy of sciences
of the Republic of Uzbekistan, Republic of Uzbekistan, Tashkent
E-mail: amkhvan@mail.ru

Zukhurova Gulnara,
Ph.D. in Technical., Senior researcher,
Institute of chemistry of plant substances Academy
of sciences of the Republic of Uzbekistan, Republic of Uzbekistan, Tashkent
E-mail: pentasolin@mail.ru

Islamova Jannat,
Ph.D. in Medical., Senior researcher,
Institute of chemistry of plant substances Academy
of sciences of the Republic of Uzbekistan, Republic of Uzbekistan, Tashkent
E-mail: islamova76@inbox.ru

Mirzakhidov Khayrulla,
Ph.D., Associate Professor, National University
of Uzbekistan, Republic of Uzbekistan, Tashkent
E-mail: muz_m77@mail.ru

COMPLEX FORMATION OF ALBENDAZOLE WITH PECTIN AND BIOLOGICAL ACTIVITY OF THE PRODUCT

Abstract. The features of the interaction of the anthelmintic drug adbendazole with citrus pectin have been studied. By the methods of potentiometric titration, viscometry, IR spectroscopy, and X-ray phase analysis it was shown that the interaction takes place in the narrow pH range using salt and hydrophobic bonds. It was established that the obtained polymer complex of albendazole "Alpec"

exhibits the more pronounced anthelmintic activity compared to the initial albendazole. It have been found that the LD_{50} of Alpec is 680 (601,8 ÷ 768,4) mg.kg $^{-1}$, which is almost 1,5 times higher than the LD_{50} of albendazole. The resulting polymer form of albendazole can be recommended for the application in medicine and veterinary practice.

Keywords: albendazole, pectin, alpec, medicine, polymer complex.

1. Introduction

The growing demand for anthelminthic medicines is caused by the extremely wide distribution of various helminths, especially in hot climates. According to WHO, at least 4 billion people are affected by parasitic diseases in the world, tens of millions of them die annually as a result of those diseases [1].

In some territories of the CIS countries, despite the success achieved in recent years in combating parasitic diseases, the epidemiological situation remains tense.

Therefore, one of the most important tasks of chemical science dealing with physiologically active compounds is the search and production of new highly effective antiparasitic drugs for medical practice.

Among the currently known anthelminthic drugs, the products belonging to the group of benzimidazole, in particular, albendazole is notable for its wide range of effects. Albendazole is characterized by a fairly high biological activity. In addition, unlike the majority of practiced drugs, albendazole is now actively used to treat such a serious disease as echinococcosis.

At the same time, albendazole, like most modern medicines, is not devoid of certain shortcomings. First of all, it is insoluble in water, which in some cases severely limits its use in medical practice.

At the same time, in the intensively developing nowadays field of chemistry of medicinal compounds it is well known that the solubility and therapeutic efficacy of known drugs can be significantly increased in many cases by their chemical modification with various high-molecular compounds. The introduction of new polymer forms of medicinal products into pharmaceutical practice, in general, can allow to control the speed and place of their absorption, give them prolonged effect, reduce toxicity, increase resistance and other valuable qualities. Polymers of both synthetic and natural origin can be used as carrier polymer. Polysaccharides, in particular, pectin, have special advantages in this respect, as it can degrade in the gastrointestinal tract and, being an enterosorbent, can simultaneously remove slags, toxins and radionuclides from the body [2–5].

2. Research purpose and objective

Given the prospects for the use of polymeric drug form of anthelminthic drug in medical and veterinary practice, this paper aims to study the peculiarities of the process of complexation of albendazole with pectin, the study of biological properties of the obtained albendazole complex to obtain a polymeric form of albendazole with increased activity.

3. Experimental part

IR spectra were shot using KBr pallets, on the FT-IR spectrometer 2000, manufactured by Perkin-Elmer (USA).

Potentiometric titration was carried out on the device I-120.0 (И-120.0) ionomer. Viscometry was carried out using Ubbelohde viscometer.

X-ray phase analysis of powders of initial components of pectin, albendazole and Alpec polymer complex was conducted on powder diffractometer ShimadzuXRD-6100 (Japan). The samples were measured in Bragg-Brentano mode with scanning of 2-θ from 4 ° to 50 °.

Albendazole produced by the Institute of the Chemistry of plant substances of the Academy of Sciences of the Republic of Uzbekistan and citrus pectin (Genu pectin typedz Manufacturer CP Kelso, lilleskensved, Denmark.) Etherification degree 58–62%, pH (1% solution) 2.9–3.4, gelling property of 145–155%, humidity not more than 12%.

The process of obtaining polymer com-plex of albendazole with pectin. The process of obtaining pectin polymer complex with albendazole. 8.34 g of albendazole was dissolved in 200 ml of distilled water, 20 ml of concentrated hydrochloric acid and 35 ml of ethyl alcohol under continuous stirring at 45–50 °C. 4.17 g pectin was dissolved separately in 237 ml of distilled water at continuous stirring. To the obtained solution of pectin at intensive stirring at 45–48 °C the prepared solution of albendazole was added 15–20 ml every 3–5 minutes and stirred for two hours [6]. Then the reaction mixture was filtered through a 0.5 mm sieve and dried on spray drying.

The range of antiparasitic action and efficiency of the investigated compounds were determined on the following experimental models of parasitosis: aspiculurosis (larval and semi-mature stage of *Aspiculuristetraptera* oxyuride) of white mice (the latter model is used as an experimental model of enterobiasis); giardiasis of white mice (vegetative forms of *Lambliamuris* and their cysts).

Efficiency of drugs was determined by the number or percentage of departing parasites – Intense Efficiency (IE). Due to the difficulty or impossibility to calculate departed parasites, the average number of helminths in exposed animals in experimental and control groups was compared and the IE (in %) was determined by the formula:

$IE = 100\ (C - O) / C$, where C is the average number of helminths in the control group; O is the average number of helminths in the experimental group.

All animals were preliminary examined for parasite infestation by coproscopy before being taken into the experiment.

During the experimental infection of mice with aspiculurosis they were injected with peros by 100 *A. tetraptera* invasive eggs. Egg excretion from the faeces of spontaneously infected mice was carried out using flotation centrifuge method. After that, the amount of suspension containing the required amount of invasive material was calculated. Only viable eggs were counted [7]. When studying the activity against larvae oxyuride chemopreparations were administered on the 5th day after aspiculurosis infection. For the study of the chemotherapeutic activity of drugs at the mature stage *A. tetrapera* the drugs were injected on the 10th day after infection. In both cases, the drugs were injected once a day, once. Accounting of the results of chemotherapy was carried out 3 days after the end of treatment by extracting and counting larvae (blind intestine) and adults (a section of the large intestine length of 10 cm) oxyuridium, using binocular magnifier MBS-1 (MBC-1) simultaneously in the experimental and control groups [8].

In experiments to determine antiprotozoic activity, white non-breeding mice of both sexes weighing 13–15 g were used. To reproduce the experimental giardiasis model, the animals were infested with oral suspension containing *Giardiamuris* $5x10^3$ cysts and trophosoites in 0.5 ml. The suspension was prepared from the content of small intestine of spontaneously infected mice (Roberts-Thomson, Mitchell method, 1978). The investigated compounds were injected into the stomach with a special atraumatic probe on the 5th day after infection within the next 5 days. All experiments were conducted in accordance with the requirements of the "European Convention for the Protection of Vertebrate Animals Used for Experimental Purposes and Other Scientific Purposes" (Strasbourg, 1986). After the end of treatment, mice were slaughtered under mild ether anesthesia by cervical dislocation and 10 cm of small intestine were taken from each animal starting with gastroduodenal articulation. The efficiency of the investigated compounds was judged by calculating the average number of vegetative forms and giardial cysts per one animal. Intense-efficacy of compounds was determined by the formula: $IE=100\ (C - O)/C$, where C is the number of trophosoites and giamblion cysts in control, O – in experiment. Examination was made at magnification 10×40 [9].

4. Results and discussion

The study of the chemical interaction of albendazole (MS) with pectin (P) was conducted by various physical and chemical methods.

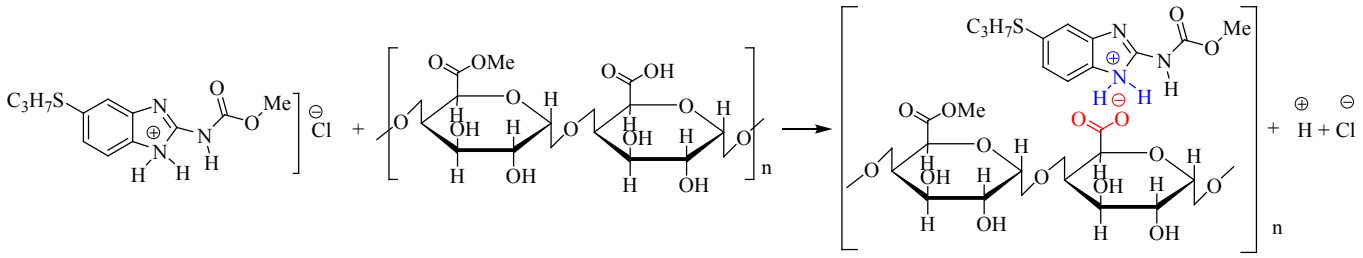

The results of potentiometric titration are shown in (Fig. 1). We can see that the addition of increasing amounts of albendazole to the aqueous solution of pectin leads to a decrease of the pH value of the medium.

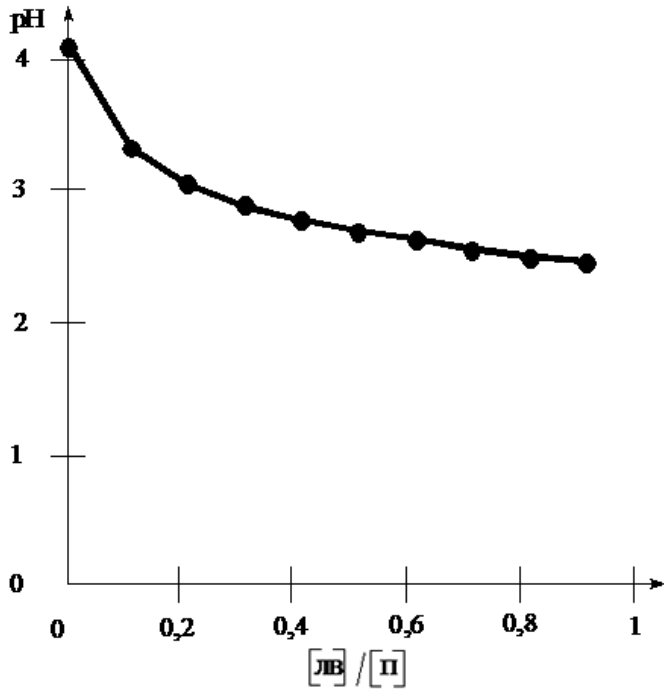

Figure 1. Dependence of medium pH changes on the ratio of [LV]/[P] components

This indicates that the process of complexation of the anthelminthic drug with the polymer is characterized by proton release according to the scheme.

According to the data of potentiometric titration the value of Θ – electrostatic bonding has been calculated. This parameter is determined by the ratio of proton concentration changes when mixing solutions of MS and polymer. As can be seen from (Fig. 2), the degree of electrostatic bonding increases with increasing content of low molecular weight MS in the solution.

It was found that the maximum degree of electrostatic bonding of albendazole to pectin is 28.2%.

One of the factors influencing the conversion depth of Θ is the medium pH environment, since the degree of electrostatic bonding of polyelectrolytes to counterions will obviously depend on the charge density on the polymer macromolecule, which is determined by the pH value of the solution.

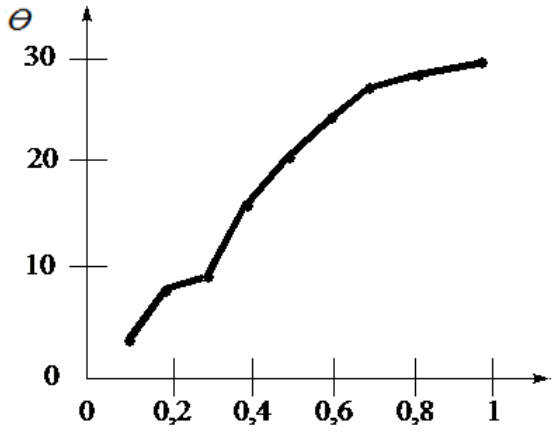

Figure 2. Dependence of electrostatic bonding (Θ) on the component ratio [LV]/[P]

Figure 3 shows the dependence of the degree of electrostatic bonding of pectin to albendazole on pH values.

From (Fig. 3) we can see that the interaction takes place in a narrow pH range of 2.3–3.3. This indicates the cooperative nature of the process of interaction between pectin and albendazole.

In albendazole-pectin system it is possible to perform both ionic and hydrophobic interaction. All this should affect the conformation state of the complex, i.e. its hydrodynamic behavior in the solution. It can be seen from (Fig. 4), that addition of increasing

amounts of MS to the ratio of 0.01 leads to a decrease of reduced viscosity of the polymer complex solution, which is explained by the implementation of a large number of ionic interactions.

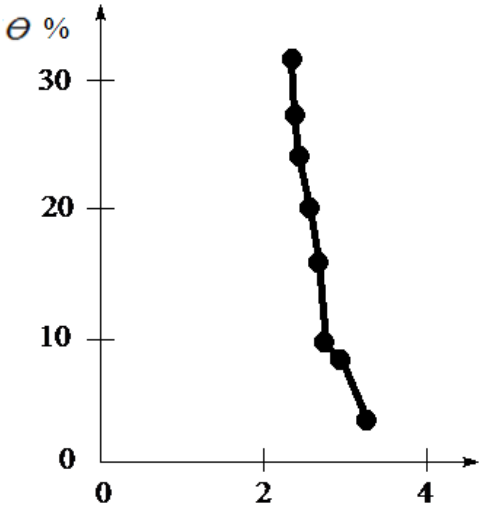

Figure 3. Dependence of the electrostatic binding parameter (θ) on pH value of the medium

However, after the ratio of 0.01 the increase of albendazole content in the polymer complex leads to the increase of its reduced viscosity and, eventually, it gels after the ratio of 0.15. This can probably be explained by the fact that hydrophobic interactions begin to prevail in the albendazole-pectin system. And eventually the polymer chains of pectin bind due to the presence of molecules between them, on the one hand, bound to the macromolecule by salt bonds, and on the other – hydrophobic to each other and the polymer.

The interaction of pectin with albendazole was also studied by infrared spectroscopy (Fig. 5). Comparison of infrared spectra of Alpec and initial components (albendazole, pectin) shows significant frequency changes in the area of double bonds and hydroxyl groups (3200–3500 cm^{-1}). A low-frequency shift of absorption bands of OH-groups of pectin (3424 cm^{-1})in the Alpec complex (3400 cm^{-1}), by 24 cm^{-1}. There is observed also a high frequency shift of C=O pectin bands (1739 cm^{-1}), in Alpec (1752 cm^{-1}), by 13 cm^{-1}. In addition, the albendazole absorption band at (1268 cm^{-1}), due to C-N bond vibrations, shifts in Alpec by 20 cm^{-1} и and is detected at (1248 cm^{-1}).

The results obtained clearly indicate the formation of albendazole polymer complex with pectin, which we call "Alpec".

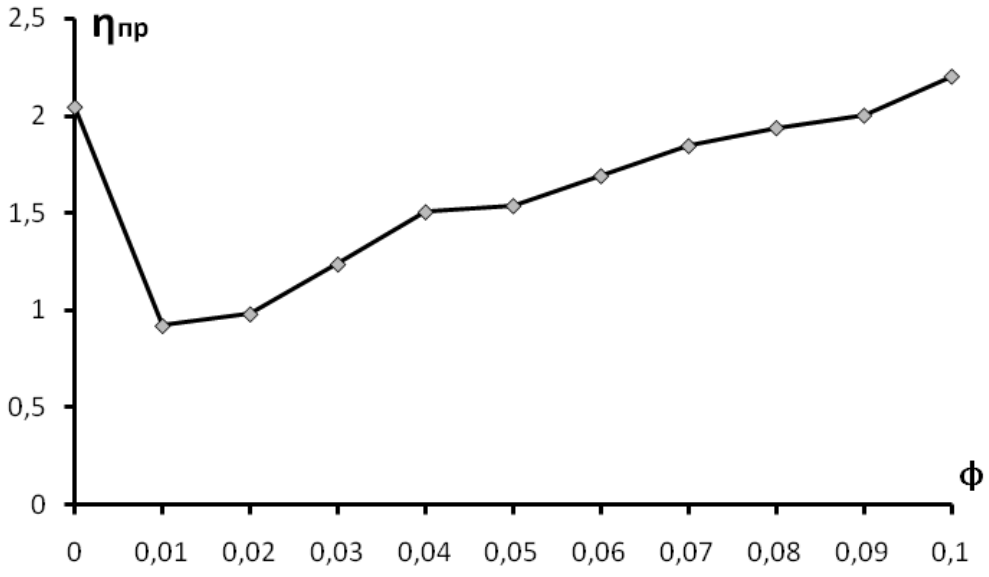

Figure 4. Dependence of the reduced viscosity of water-alcohol (1:1) solutions of albendazole polymer complex with pectin on the ratio. φ=[Albendazole]/[Pectin]. T = 303 °C

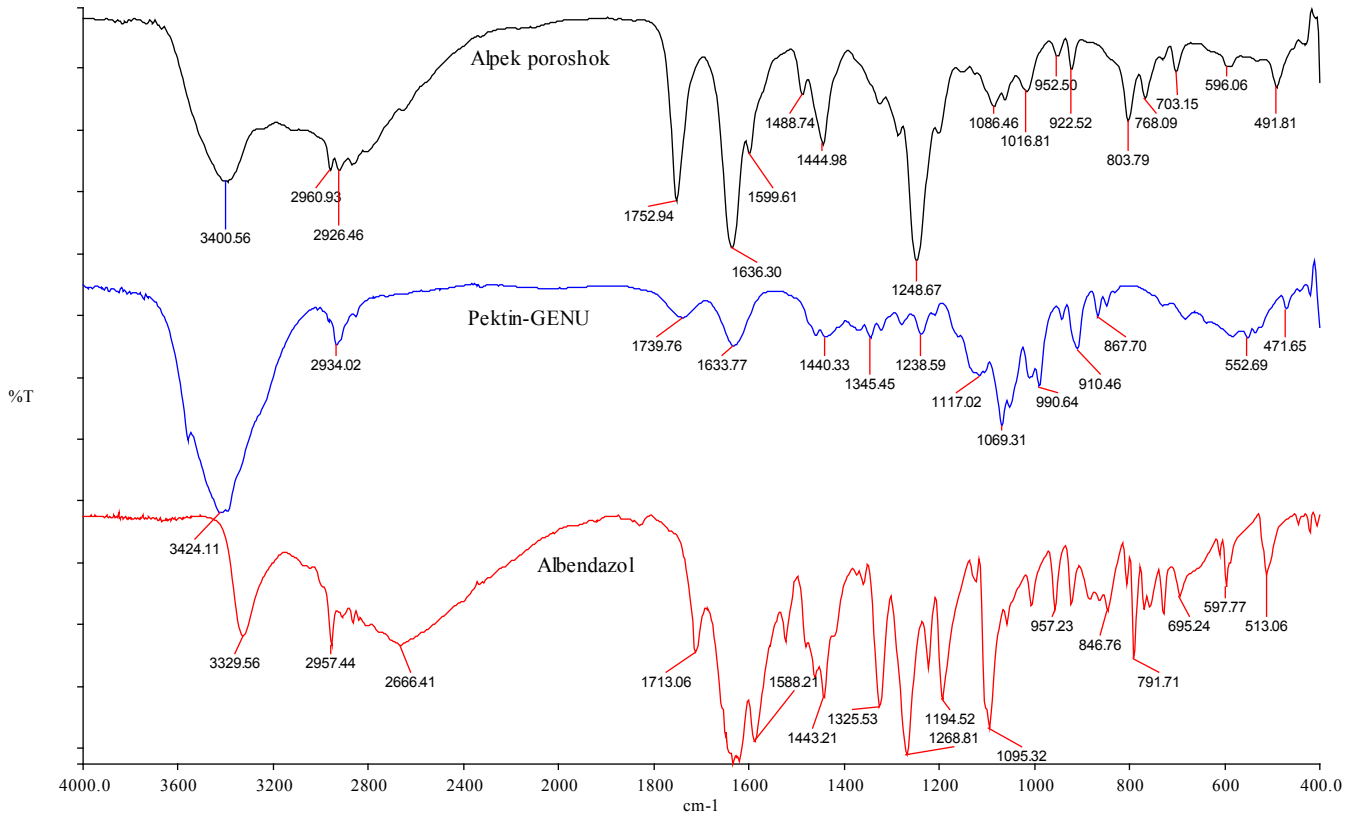

Figure 5. IR spectra of albendazole, pectin-GENU, albendazole complex with pectin (Alpec)

The formation of polymer complex as a result of interaction of albendazole with pectin was also studied by X-ray phase analysis (Fig. 6).

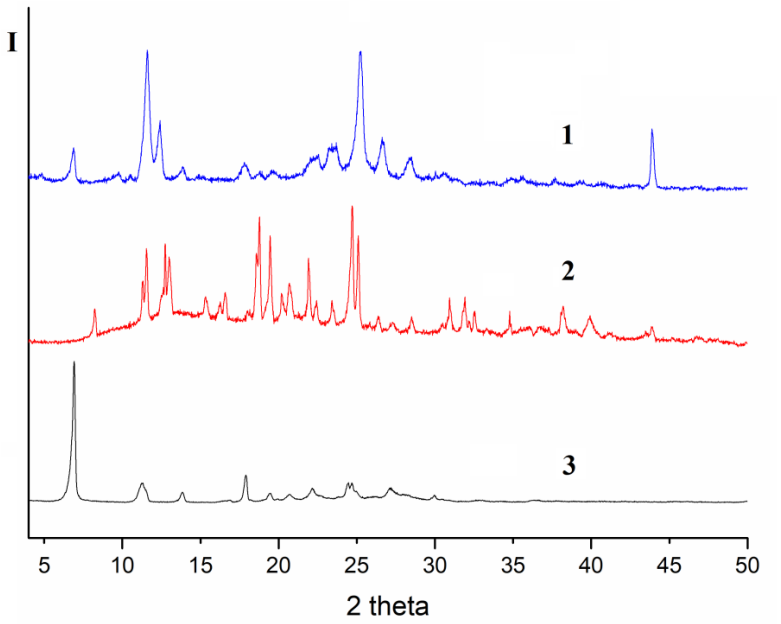

Figure 6. Comparison of X-ray diffractograms of Alpec (1) with pectin (2) and albendazole (3)

On the diffractogram of the pectin complex with albendazole one can see new diffraction peaks at 4.84°, 9.73°, 10.48°, 11.60°, 12.42° and other 2-θ angles, at which diffraction peaks of initial albendazole and pectin are not observed, that testifies to the formation of a crystal lattice of the complex, which differs from albendazole and pectin. It is also seen that the amorphous peak of pectin with the center at 13.68° is not observed on the diffractogram of the complex, which means that the amorphous part of the pectin passes into the crystal structure of the complex.

Thus, the comparative X-ray phase analysis of albendazole, pectin and Alpec confirms the formation of Alpec polymer complex with a new crystal lattice.

Biological studies of anthelminthic activity of albendazole polymer complex with pectin Alpec were carried out on an experimental model of aspiculurosis. The results obtained indicate that Alpec has the pronounced antinematodetic aaction against mature stage of *A. tetraptera* already in a dose 2 times lower than the albendazole itself.

The study of the protozoic activity of the giardiasis model of white mice also revealed a pronounced antigirardiasis effect of Alpec, which is superior to that of albendazole, too.

The increased biological activity of Alpec can probably be explained by the good water solubility of Alpec unlike albendazole, which, as a consequence, leads to increased bioavailability of the preparation.

On the experimental model of aspicululosis the administration of drugs at the sexually mature stage *A. tetraptera* showed the expressed activity of albendazole complex with pectin (Table 1).

Table 1.– Results of the study on the efficacy of alpec efficiency on the semiadult stage of *A. tetraptera* development (in comparison with albendazole)

Drug	Dose mg·kg $^{-1}$, n = 6, once	The number of parasites after autopsy	Intense Efficiency,%
"Alpec"	2.5	5.2 ± 0.38*,**	91.4
	5	4.0 ± 0.58*,**	93.4
	10	3.6 ± 0.8*,**	94.1
Albendazole	2.5	15.6 ± 1.2*,**	74.2
	5	6.0 ± 0.36*	90.1
	10	5.0 ± 0.44*	91.7
Control	–	60.8 ± 2.2	–

*Note: * – accurate with control; ** – accurate with comparative drug effect ($p < 0.05$)*

The dose of Alpec 5 mg·kg $^{-1}$ was 93.4% effective, while albendazole in this dose was 90.1%. With the increase of the dose up to 10 mg·kg $^{-1}$ the efficacy of Alpec remained almost unchanged (94.1%), but it was higher than that of albendazole (91.7%) in the same dose (Table 1).

Table 2.– Results of the study on the antigirardiasis effect of Alpec (in comparison with albendazole)

Drug	Dose mg·kg $^{-1}$, n=6, for 5 days	The number of parasites after autopsy.	Intense Efficiency,%
1	***2***	***3***	***4***
Alpec	2.5	402.3 ± 2.2*	81.0
	5	324.7 ± 3.4*,**	84.7
	10	315.5 ± 1.2*,**	85.2

1	*2*	*3*	*4*
Albendazole	2.5	784 ± 29.2*,**	6.1
	5	412.6 ± 2.1*	80.6
	10	400.4 ± 2.3*	81.2
Control	–	2125.8 ± 121.2	–

*Note: * – accurate with control; ** – accurate with comparative drug effect ($p < 0.05$)*

Therefore, Alpec has an antinomatose effect on *A. tetrapetra* in a dosage 2 times lower than that of albendazole itself.

The antiprotozoic effect of Alpec was studied on the model of giardiasis of white mice (vegetative forms of *Lambliamuris* and their cysts).

The evident antigirardiasis effect of albendazole complex with pectin as the studied drug was observed when administered for 5 days in a dose of 5 mg·kg^{-1} with *IE* = 84.7% (table 2).

The result of a 2-fold increase in dose (10 mg·kg^{-1}) – resulted in a slight change of 85.2%, respectively. The dose of 2.5 mg·kg^{-1} can also be considered quite effective – 81.0%. All this data indicates the high antiprotozoic activity of the test Albendazole complex with pectin in an optimal dose of 5 mg·kg^{-1}. Comparison of Alpec with the initial albendazole showed that it is significantly more active than the latter latter as the reference drug in the same dose.

The study of acute toxicity of Alpec was carried out in experiments on white pedigree rats weighing 210–250 grams. The average lethal dose of Alpec (LD_{50}), was determined, it is – 680 (601.8÷768.4) mg·kg^{-1} (LD_{50} of albendazole – 400.2÷450.4) mg·kg^{-1}), i.e. the polymeric complex of Alpec is classified as moderately dangerous in terms of parameters of acute toxicity for intragastric use.

4. Conclusion

The interaction of albendazole with pectin was investigated by potentiometry, viscometry, infrared spectroscopy and X-ray phase analysis methods. It was shown that the interaction takes place with the help of salt and hydrophobic bonds to form a polymer complex (Alpec). High antiparasitic (more pronounced antinematodetic than antigirardiasis) activity of Alpec as compared to the original albendazole was detected, which is probably explained by an increase of the solubility of the drug and, consequently, by its increased bioavailability. It was found that in terms of "acute" toxicity index, the "Alpec" complex exceeds the initial albendazole by almost 1.5 times.

The obtained polymeric complex Alpec can be recommended for the use in medical and veterinary practice.

Список литературы:

1. Думбадзе О. С. Паразитарные заболевания: практические рекомендации врача-инфекциониста. Специализированный медицинский журнал. Главный врач юга России. 2007.– № 4(12).– С. 40–42.
2. Панарин Е. Ф. Полимеры в медицине и фармации: Е. Ф. Панарин.– СПб.: Изд-во Политехн. ун-та, 2008.– С. 81–91.
3. Штильман М. И. Полимеры медико-биологического назначения.– Москва.– Академкнига. 2006.– С. 15–239.
4. Хван А. М., Абдуазимов Х. А. Взаимодействие лигносульфата с антигельминтным препаратом медамин. Хим. Прир. Соед. 1999.– № 5.– С. 682–684.
5. Сарымсаков А. А., Рашидова С. Ш. Перспективы создания полимерных лекарственных препаратов с наноструктурой. Труды ИХФП АН РУз. 2011.– С. 225–235.

6. Zukhurova G. V., Sadikov T., Makhmudova B. Sh., Eshimbetov A. G., Abdurazakov A. Sh., Sagdullaev Sh. Sh. 11th International Symposium on the Chemistry of Natural Compounds. 1–4 October, 2015. – Antalya, Turkey. Quantitative determination of the major substance In the preparation alpec. – 157 p.
7. Лыкова Н. И. Медико-биологическое обоснование использования моделей Aspiculuristetraptera и Syphaciaobvelata для поиска и создания новых препаратов. Афтореф. дис. канд. биолог. наук.– Москва, 1994.
8. Хабриев Р. У. Руководство по экспериментальному (доклиническому) изучению новых фармакологических веществ.– Москва. Медицина, 2005.– 593 с.
9. Ириков О. А., Коваленко Ф. П. Экспериментальная модель активированной инфекции Lamblia (Giardia) muris белых мышей. Мед. паразитол. и паразитарные болезни. издательство С-ИНФО – Москва. 2007.– № 3.– С. 7–11.

https://doi.org/10.29013/AJT-20-3.4-32-38

Kaypnazarov Turdibay Nzamatdinovich,
Junior Researcher. S. Yu. Yunusov
Institute of the Chemistry of Plant Substances AS Uzbekistan,
Tashkent, Uzbekistan
E-mail: kturdibay1@mail.ru

Ramazonov Nurmurod Sheralievich,
Doktor of Chemical Sciences. S. Yu. Yunusov Institute
of the Chemistry of Plant Substances AS Uzbekistan,
Tashkent, Uzbekistan

Egamova Feruza Rustamovna,
Junior Researcher. S. Yu. Yunusov
Institute of the Chemistry of Plant Substances AS Uzbekistan,
Tashkent, Uzbekistan

Khushbaktova Zaynab Abduraxmanovna,
Doktor of Medical Sciences. S. Yu. Yunusov
Institute of the Chemistry of Plant Substances AS Uzbekistan,
Tashkent, Uzbekistan

Sirov Vladimir Nikolaevich,
Doktor of Medical Sciences.S.Yu.Yunusov
Institute of the Chemistry of Plant Substances AS Uzbekistan,
Tashkent, Uzbekistan

ISOLATION AND STUDY OF EFFECT OF CYCLOARTAN GLYCOSIDES ON METABOLIC PROCESSES IN CARDIAC MUSCLE OF EXPERIMENTAL ANIMALS

Abstract. The paper describes the preparation of Astragalus janischewskyi extract and defines cycloartane glycosides. Experimentally in male rats (180–200 g), 10 daily oral administration of this extract (10 mg/kg) and riboxine (50 mg/kg) has been found to promote the activation of metabolic processes in cardiac muscle. In terms of the effect on carbohydrate-energy and lipid exchanges, the tested extract Astragalus janischewskyi is not inferior to riboxine, in terms of antioxidant action it is reliably superior to the effect of the reference preparation used.

Keywords: Astragalus, cycloartane glycosides, qualitative and quantitative analysis, metabolic processes.

Introduction: Genus Astragalus, cem. Leguminosae, has about 2.500 species and in this regard has no equal among flowering plants. This genus is also one of the largest in the flora of Central Asia. In the territory of the Republic of Uzbekistan, 254 species of this plant grow [1].

Many plants of the genus Astragalus containing cycloartane triterpenoids (cycloartane glycosides) have long been widely used in folk and waitinal medical practice as sufficiently effective cardiotropic agents [2; 3; 4]. This report analyzes the effects of Astragalus janischewskyi Popov extract on the state of certain metabolic processes in the heart muscle that ultimately determine its functional activity. Experiments were carried out in comparison with the known preparation riboxine, which has a positive effect on myocardial metabolism and is applied due to this in myocardiodystrophy, ischemic heart disease and in some other forms of cardiac pathology [5].

Experimental chemical part. The dried ground surface portion (1 kg) of the Astragalus janischewskyi Popov plant was used. Leguminosae [6] harvested in June 2019 in Surkhandarya region. Extraction was carried out with methyl alcohol (4 L) at room temperature 25 ºC for 24 hours under periodic shaking (5 times). Extract was concentrated under reduced pressure and temperature 40–50 ºC to consistency of thick resinous mass. Distilled water (300 ml) was added to the initial resinous mass obtained after the primary (methanol) extraction (38 g), and a coloured homogeneous solution was obtained with vigorous stirring. The aqueous solution was then extracted successively with chloroform, ethyl acetate and n-butyl alcohol. Extraction uparit dry. 21.5 g of butanol recovery were obtained.

The presence of cycloartane triterpenoids was carried out by thin layer chromatography on "Silufol" plates in solvent systems: chloroform-methanol-water (4: 1: 0.1; 70: 23: 3; 60: 35: 5). Chromatography of alcohol extracts was carried out with samples of previously known cycloartanes. After chromatography, it was sprayed with a 20% alcohol solution of phosphoronolphramic acid, then heated in an oven for 8–10 minutes at 100 °C. The adsorption zones of cycloartane substances and witnesses were colored brown.

The sum of the extractive substances was then diluted (100 ml) with n-butyl alcohol. The concentrated alcohol solution on the Schott funnel was eluted through an alumina layer (neutral, Brockman type II). The butanol solution obtained after multiple elution through the adsorbent layer was concentrated to dryness under reduced pressure at a temperature not higher than 70 °C. A crystalline mass was obtained in an amount of 7.75 g (36% based on the amount (21.5 g) of the starting resinous mass).

Column chromatography was performed on KSK silica gel using the chloroform-methanol-water solvent system (9:1:0.01; 6:1:0.05; 70:12:0.1; 70:23:3). As a result, four glycosidic substances were obtained. These compounds were the previously described cyclosiversiosides E, F, G and astragoloside VII.

Quantitative analysis of astragoloside VII was also carried out by HETLC using external standards.

To prepare the samples, 1 mg of the substance or test mixture was dissolved in 1 ml of methanol. Applied on a chromatographic plate on 3: l solution by means of Linomat 5. The latitude of the tracks is 3 mm, the distance between them is 7 mm.

Sigma-Aldrich silica gel on TLCAL foilsl (Germany) chromatography plates were used for analysis.

Solvent systems: chloroform: methanol: water – 70: 15: 0.1 were used as eluant. Elution was carried out in a glass chamber (distance 7 cm). The plates were air-dried after elution for 15 minutes and developed with 20% alcohol solution of phosphoronolphramic acid, then heated in an oven for 8–10 minutes at 100 °C. The adsorption zones of cycloartane substances and astragoloside VII were colored brown.

Chromatography was performed at room temperature on a CAMMAG TLC SCANNER3 instrument. UV detection at wavelengths 400 nm.

The content of astragoloside VII (x) in the sample was calculated by the formula:

$$x = \frac{C_{std} \times S_{sub} \times M_{sub}}{S_{std} \times C_{sub}}$$

Where:

C_{std} – is the concentration of the standard solution (mg/ml);

S_{sub} – is the area of the substance peak in the substance (3655.6);

M_{sub} – is the mass of the crystalline substance (7.75 g).

S_{std} – is the peak area of the substance in standard solution (20749);

C_{sub} – is the concentration of the substance solution (mg/ml);

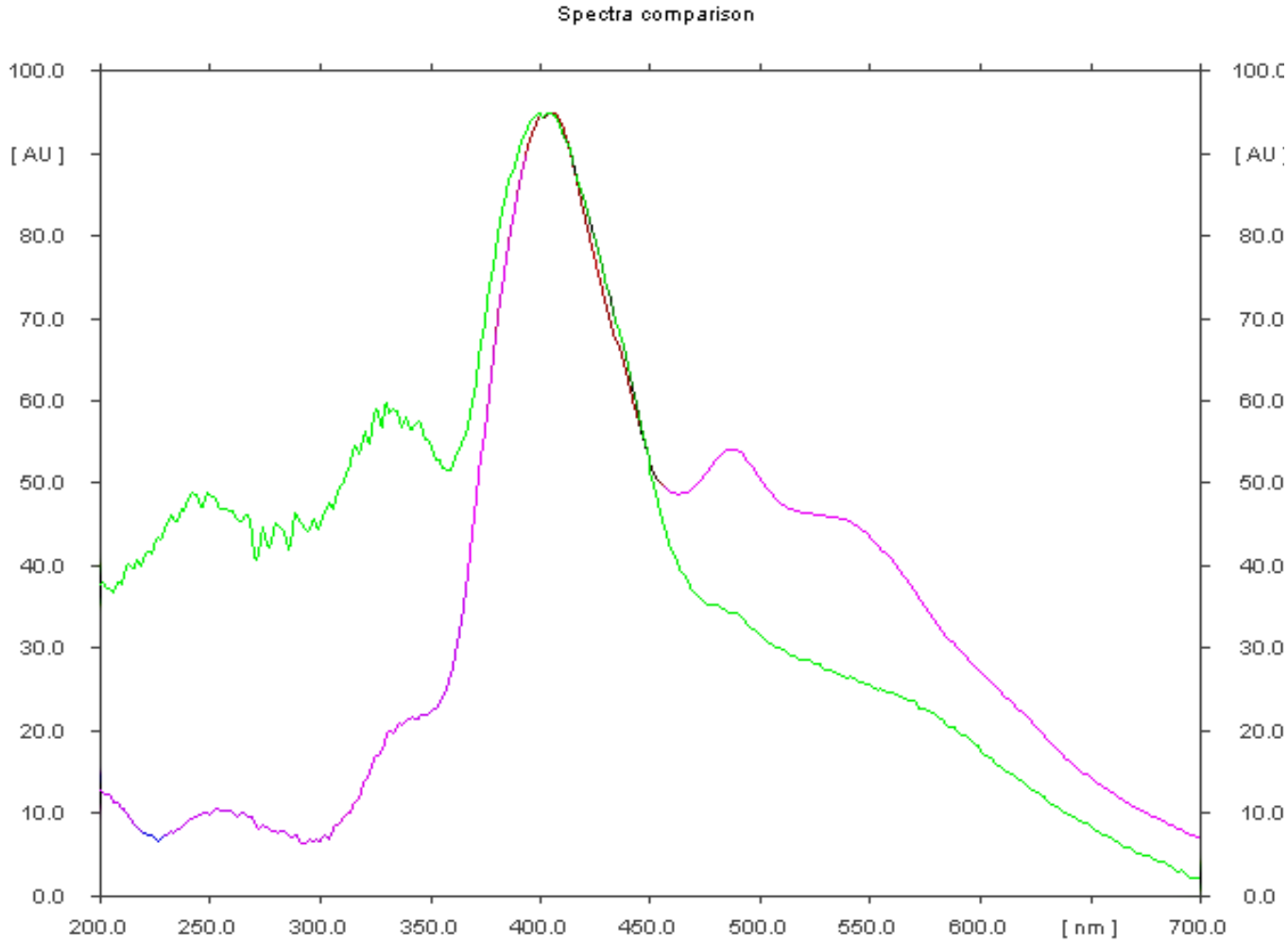

Figure 1. HETL chromatogram astragoloside VII and the sum of cycloartane glycosides

Cyclosiversioside E (1) [7]. 80 mg of compound of composition $C_{40}H_{66}O_{13}$ was isolated, mp 252–254 °C (from methanol).

NMR spectrum 1H(400 MHz, C_5D_5N, δ, ppm, J/Hz, 0-TMS): 0.42 and 0.48(2H-19, d,^{2}J=4.95 of Hz), 0.97, 1.16, 1.18, 1.29, 1.45, 1.66 and 1.80(d, 7 × × CH_3), 3.32 (1H, dd,^{3}J = 11.74 and 4.44 Hz, H-3), 3.75 (1H, td,^{3}J = 8.95 and 5.29, H-6), 2.58(1H, d,^{3}J=7.8 of Hz, H-22), 3.91(1H, dd,^{3}J=8.24 and 7.34 H-24), 4.69(1H, d,^{3}J=7.45 of Hz, Xyl*p* H-1′), 4.76 (1H, d,^{3}J=7.28 of Hz, H-1′′ Xyl*p*).

Cyclosiversioside F (2) [8]. 50 mg of compound of composition $C_{41}H_{68}O_{14}$ was isolated, mp 260–261 °C (from methanol).

NMR spectrum 1H (400 MHz, C_5D_5N, δ, ppm, J/Hz, 0-TMS): 0.42 and 0.48(2H-19, A,^{2}J=4.51 of Hz), 0.97, 1.16, 1.18, 1.25, 1.45, 1.80 and 1.99(d, 7×CH_3), 3.32 (1H, dd,^{3}J=11.79 and 4.28 Hz, H-3), 3.75 (1H, td,^{3}J=8.88 and 5.30, H-6), 2.56 (1H, d,^{3}J=9.04 of Hz, H-22), 3.92 (1H, dd,^{3}J=8.26 and 7.01 H-24), 4.69(1H, d,^{3}J=7.45 of Hz, Xyl*p* H-1′), 4.76(1H, d,^{3}J=7.30 of Hz, H-1′′ Glc*p*).

Cyclosiversioside G (3) [9]. 45 mg of the compound of composition $C_{46}H_{76}O_{17}$ was isolated, mp 226–228 °C (from methanol).

Range of nuclear magnetic resonance 1H (400 MHz, $CDCl_3$ CD_3OD, δ, m of, J/Hz, 0-TMC): 0.18 and 0.48 (2H-19, dd,^{2}J = 4.54 Hz), 0.95. 1.07. 1.14. 1.17. 1.18. 1.20 and 1.21 (d, 7 × CH3), 3.08 (1H, dd,^{3}J = 9.65 and 3.56 Hz, H-3), 3.46 (1H, td,^{3}J = =8.70 and 3.53, H-6), 2.30 (1H, d,^{3}J = 7.85 Hz, H-22), 3.77 (1H, dd,^{3}J = 5.17 and 4.98 H-24), 4.59 (1H, d,^{3}J = 7.20 Hz, H-1′ Xyl*p*), 4.61 (1H, d,^{3}J = = 7.56 Hz, H-1″ Xyl*p*), 4.31 (1H, d,^{3}J = 6.74 Hz, H′-1′ Rha*p*).

Astragoloside VII (4) [10]. 230 mg of compound of composition $C_{47}H_{78}O_{19}$ was isolated, mp 291–292 °C (from methanol).

NMR spectrum 1H (400 MHz, C_5D_5N, δ, ppm, J/Hz, 0-TMS): 0.18 and 0.56(2H-19, dd,^{2}J = 4 Hz), 0.90. 1.24. 1.34. 1.37. 1.38. 1.60 and 2.01 (s, 7×CH3), 3.50 (1H, dd,^{3}J = 11.79 and 4.44 Hz, H-3), 3.76 (1H, td,^{3}J = 8.95 and 5.30, H-6), 2.77 (1H, k,^{2}J =$^3J_1$ =$^3J_2$ = 11.04 Hz, H-22), 3.50 (1H, dd,^{3}J = 8.26 and 7.31 H-24), 4.89 (1H, d,^{3}J = 7.75 Hz, H-1′ Xyl*p*), 4.86 (1H, d,^{3}J = 8.10 Hz, H-1″ Glc*p*), 5.06 (1H, d,^{3}J = 8.05 Hz, H-1‴ Glc*p*).

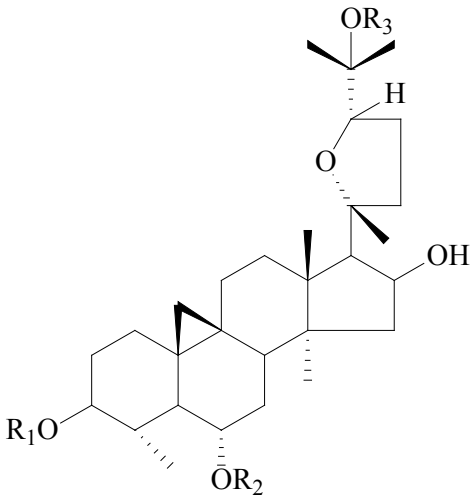

R_1= R_2=Xyl*p*, R_3=OH

R_1=Xyl*p*, R_2=Glc*p*, R_3=OH

R_1=Rha*p*(–2-Xyl*p*), R_2=Xyl*p*, R_3=OH

R_1=Xyl*p*, R_2= R_3=Glc*p*

Experimental biological part. Biological experiments were performed on male rats weighing 180–200 g. The extract of Astragalus janischewskyi containing the sum of said cycloartan glycosides (EA) was administered orally at a dose of 10 mg/kg for 10 days. At the end of this period, animals were killed by instant decapitation under mild essential anesthesia. The heart was extracted and used for biochemical studies. Glycogen was determined by Lo S. et.al (1970), lactic and pyruvic acids (MK and PVC) were determined by the methods of Gutman I., Wahlefeld A. W. and Friedeman F., Haugen G. E. (1974; 1943). The redox potential of the milk-pyruvic acid system (M.C./PVK OBP) was calculated by Raiskin M. E. et al. (1970), adenine nucleotides were determined by paper descending chromatography by Wencstern T. V. and Baev A. A. (1957). Content of cholesterol, triglycerides, phospholipids and not esterified fatty acids defined as it is described in [7], low-new dialdehyde (MDA) according to Steel I. D. and Garishvili T. G. (1977), catalases on Korolyuk M. A., etc. (1988), superoxide dismutases (SOD) according to Dubinina E. E., etc. (1982) and catalases on Korolyuk M. A., etc. (1983).

Statistical processing of the obtained data was carried out by the method of variation statistics with assessment of reliability of differences between control and experimental groups using Student ‘s t-criterion.

Results and their discussion. Studies have shown that ten days of EA administration has a

positive effect on carbohydrate metabolism in myocardium. Under its influence glycogen content increased by 27.7%, PVK content increased by 23.6%, MK content, on the contrary, decreased by 15.8%. As a result, the MK/PVK ORP increased by 5.1 mV. Increase of glycogen level under the action of EA and increase of redox potential of milk-pyruvic acid system in myocardium indicates the prevalence of aerobiosis processes in this case (Table 1). These data have already indicated an increase in the energy input of cardiomyocytes.

However, it was further confirmed that the ATP content of the myocardium was increased by 25% upon multiple administration of EA to animals, the ADF content was not significantly changed, and the AMP level was decreased by 15.4%. Therefore, the ratio of ATP/ADP to ATP/AMP increased by 21.4 and 47.7%. The sum of adenine nucleotides in the myocardium increased by 14.8%. The energy charge of the system increased by 5.3%. The detected changes in the ratio of adenine nucleotides indicate the prevalence of synthesis processes over macroergues recycling processes (Table 1).

Table 1.– Effect of Astragalus janischewskyi plant extract on the metabolite content of energy metabolism in the heart muscle of rats (M ± m, n = 6)

Expriments medium	Intact animals	Extract of *Astragalus*	Riboxin
Glycogen, mg%	282 ± 12.2	360 ± 16.4*	330 ± 14.6*
Pyruvic acid (PA), mg%	1.48 ± 0.06	1.83 ± 0.08	1.76 ± 0.05
Lactic acid (LA), mg%	52.6 ± 2.4	44.3 ± 2.2*	45.6 ± 1.8*
Relatively recovery potential of the system LA/PA, millivolt	–251.6	–246.5	–247.4
Adenosine triphosphoric acid (ATPh), micromole/gramme	2.32 ± 0.06	2.90 ± 0.12*	2.76 ± 0.10*
Adenosine diphosphoric acid (ADPh), micromole/gramme	0.68 ± 0.03	0.70 ± 0.03*	0.70 ± 0.04
Adenosine monophosphoric acid (AMPh), micromole/gramme	0.52 ± 0.02	0.44 ± 0.02*	0.46 ± 0.01*
ATPh/ADPh	3.41 ± 0.20	4.14 ± 0.22*	3.94 ± 0.18*
ATPh/AMPh	4.46 ± 0.24	6.59 ± 0.32*	6.00 ± 0.28*
Sum of adenine nucletides	3.52 ± 0.08	4.04 ± 0.12*	3.92 ± 0.102*
Energy charge	0.76 ± 0.007	0.80 ± 0.01*	0.79 ± 0.005*

Note: Reliability with respect to the corresponding indicators of intact animals (reliability level is accepted at $p < 0.05$)

Table 1 also shows that EA, by its effect on the carbohydrate-energy metabolism of the heart muscle, acted similarly to the comparison preparation riboxine, although in some cases it exhibited a more distinct effect. Thus, when riboxine was administered to animals, glycogen and PVK content in the heart increased by only 17.0 and 18.9%, MK decreased by 13.3%. The MC/PVK ORP increased by 4.2 mV. The sum of adenine nucleotides increased by 11.4% and the energy charge of the system increased by 3.9%.

The effects of EA and riboxine on the lipid content of the myocardium were also similar. Under their influence, cholesterol content decreased by 17.1–16.8 ($p < 0.05$), triglycerides by 15.9–14.0 ($p < 0.05$), and NEGA by 20.5–27.0% ($p < 0.05$). Phospholipid content increased by 21.7–19.8% ($p < 0.05$). At the same time, the effectiveness of

EA and riboxine varied significantly when considering their effects on the activity of the body 's antioxidant protection enzymes and lipid peroxidation processes. It can be seen from Table 2 that the administration of EA increases the activity of the key enzymes of the antioxidant system.

Catalase activity in the heart muscle under its influence increased by 27.3% and SOD activity by 17.7% relative to intact animals.

Riboxine contributed to an increase of only 9.1 and 9.8% in the activity of these enzymes in the myocardium.

Table 2.– Effect of Astragalus janischewskyi plant extract on activity of body antioxidant protection enzymes and lipid peroxidation processes (M ± m, n = 6)

Experiment medium	**Katalaza mkat/min/g protein**	**Superoxide dismutase conventional units/ min/mg/ protein**	**Raspberry dialdehide nmol/mg protein**
Intact animals	13.2 ± 0.52	0.620 ± 0.008	0.280 ± 0.022
Extract of *Astragalus janischewskyi*	16.8 ± 0.64*.1	0.730 ± 0.009*.1	0.150 ± 0.010*1
Riboxin	14.4 ± 0.58	0.680 ± 0.006*	0.190 ± 0.012*

*Note: * – Reliability with respect to the corresponding indicators of intact animals; 1 is the level of validity between groups of animals treated with EA and riboxine (p < 0.05)*

The level of one of the end products of lipid peroxidation – MDA in the heart of animals treated with EA decreased by 46.4 and those treated with riboxin – 32.1%. The difference in activity of antioxidant protection enzymes in the heart muscle of rats treated with EA and riboxine was in all cases significant.

Thus, in the experiments carried out, it was found that the tested extract Astragalus janischewskyi on activating effect on carbohydrate-energy and lipid metabolism of heart muscle in healthy animals is not inferior to the effect of riboxin, but in its antioxidant effect it is reliably superior to the reference preparation used in practice.

References:

1. Flora SSSR.– M.-L.: AN USSR, 1946.– T. 12.– 918 p.
2. Kamedin R. V. Astragalus L., Astragal. Opredelitel rasteniy Sredney Azii. – Tashkent. Izdatelstvo "Fan", UzSSR,– T. 6.– 211 p.
3. Dornikova N. P. Ob izmenenii pokazateley krovoobrascheniya v zhiznenno vazhnykh organakh na rannikh etapakh pazvitiya gipertonicheskoy bolezni pri lechenii bolnykh pushistotsvetkovym astragalom: avtoreferat dis. Doktora med. nauk.– Dnepropetrovsk, 1974.– 35 p.
4. Kisileva T. L. Astragal // Med. sestra. 1991.– No. 8.– P. 49–51.
5. Li S. Q., Ynan R. X., Wang Y. Q. Clinical observation on treatment of ischemic heart disease with Astragalus membranaceus // Chin. J. Integr Trad Western Med. 1995.– No. 15.– P. 77–80.
6. Flora Uzbekistana. – Tashkent: AN UzSSR, 1955.– T. 3.– 537 p.
7. Naubeev T. Kh. and Uteniyazov K. K. // Structure of cyclochivinoside C from Astragalus chivensis, Chemistry of Natural Compounds,– Vol. 43.– No. 5. 2007.
8. Kaypnazarov T. N., Uteniyazov K. K. and Saatov Z., Triterpene glycosides from Tragacantha stipulosa and their genins. Structure of cyclostipuloside E // Chemistry of Natural Compounds,– Vol. 40.– No. 1. 2004.– P. 40–44.

9. Svechnikova A. N., Umarova R. U., Gorovits M. B., Adullayev N. D., Abubakirov N. K. Triterpenovyye glikozidy Astragalus i ikh geniny. XI. Tsiklosiversiozid G – thiglikozid iz Astragalus sieversianus // Khimiya prirod. soyedin.– Tashkent, 1983.– No. 3.– P. 312–321.
10. Kitagawa I., Wang H., Yoshikawa M., Saponin and sapogtnol. XXXVII. Chemical constituents of Astragali Radix, the root of Astragalus membranaseus Bunge. (4). Astragalosides VII and VIII // 1983.– V. 31.– P. 716–722.
11. Mashkovsky M. D. Lekarstvennyye sredstva.– Tashkent. Izdatelstvo med. Lireratury im. Abu Ali ibn Sino, 1998.– T. 2.– P. 173–174.
12. Kamyshnikov V. S. Spravochnik po kliniko-biokhimicheskim issledovaniyam i laboratornoy diagnostike.– M.: MED press-inform, 2009.– 896 p.

https://doi.org/10.29013/AJT-20-3.4-39-45

Tilavov Khusan Shomurodovich,
Doctoral student of Tashkent Institute of Chemical Technology
Sarsenbaev Nurlan Tenelbayuly,
Master of the Tashkent Institute of Chemical Technology
Kadirov Khasan Irgashevich,
Doctor of technical sciences,
Professor, Tashkent Institute of Chemical Technology
E-mail: tkti.kodirov@mail.ru
Baltabaev Ulugbek Narbaevich,
Doctor of technical sciences(PhD).,
associate professor,
Tashkent Institute of Chemical Technology

PYRIDINE BASE SYNTHESIS CATALYSTS

Abstract. The aim of this work was to obtain corrosion inhibitors. It has been established that heterocyclic compounds, including pyridine and its derivatives, are used more and more often as the active component in the composition of modern corrosion inhibitors. The catalytic reaction of obtaining pyridine and its derivatives by passing a mixture of acetaldehyde and formalin with ammonia was studied. The resulting catalyst in the mixture was used as an inhibitor of hydrochloric acid treatment.

Keywords: heterocyclic compounds, pyridine, catalyst, corrosion inhibitor, acetylene, ammonia.

Introduction. The accelerated development of the oil and gas industry has an impact on scientific and technological progress in the field of engineering and technology for drilling, production, transportation and processing of oil and gas.

An increase in the number of people involved in the development of new gas, gas condensate and oil fields, the introduction of oil and gas pipelines and compressor and economic methods and technical means to prevent the occurrence of corrosion effects on borehole, field, transport equipment and pipelines. Natural gas contains highly corrosive components, such as hydrogen sulfide (1.0–5.0% vol.) and carbon dioxide (up to 6% vol.).

The fight against corrosion of oil and gas equipment is carried out by various methods [1; 2]. However, the most widely used inhibition is one of the simplest, most effective and economically feasible methods of combating corrosion.

Corrosion inhibitors inhibit, and in some cases almost completely allow the process of destruction of metals in aggressive environments, acting as a protective coating and neutralizer.

Currently, Dodicor (Germany), Danox (Spain), Vikor, Neftekhim-3, V-2, V-3 (Russia) and others are used as a corrosion inhibitor in the Republic [3].

The procus of increasing of new substances with inhibition properties continues intensively, among which heterocyclic compounds have their own special place.

The authors of [4] studied the inhibitory capabilities of some heteroaromatic bases and their complexes with transition metal salts, as well as the development of effective corrosion inhibitors in order to protect the equipment of the petrochemical and oil-gas field complexes.

I. V. Kolobova revealed the protective effect of nitrogen-containing compounds and complexes

with transition metal salts. Preliminary tests of the inhibitory ability of pyridines and quinolines were carried out using a Monicor-1M corrosion meter in a 5% aqueous NaCl solution in a three electrode cell under stirring of a corrosive medium. At the same time, it was found that 4-vinylpyridine, pyridinothiols of 2- [beta] -oxyethylpyridines in high concentrations noticeably reduces the rate of corrosion of metal St.20.

In works [5–7], universal corrosion inhibitors based on aminophenols and heterocyclic amines of the "SNPH" brand are proposed. For this, a series of functionally substituted alkyl- [poly- (ethyleneoxy)] – phosphoryl pyridine, alkyl- [poly- (ethyleneoxy)] – phosphorylquinoline, aryl- [poly- (ethyleneoxy)] – phosphoryl pyridine and aryl- [poly- (ethyleneoxy) series was synthesized.)] – phosphorylquinoline salts and systematic studies of their properties were carried out. It was found that a number of synthesized compounds have high anticorrosive properties in highly mineralized hydrogen sulfide and carbon dioxide containing aqueous media, as well as the dependence of the anticorrosive activity of the synthesized compounds on the length of the alkyl substituent in the alkyl and aryl radical, and the degree of hydroxyethylation. The dependence of the anticorrosive action of the synthesized compounds on concentration and time was studied. Using IR spectroscopy, it was shown that the phosphoryl group present in the structure of the synthesized compounds ensures the chemisorption of inhibitor molecules on the metal surface due to the formation of complex compounds with iron (II) ions. Using probe electron microscopy, it was found that the synthesized heterilonium salts form an adsorption film on the metal surface, which prevents corrosion damage. Given the high cost and the impossibility of using individual heterocyclic amines for large-scale production, the synthesis of the corresponding heterilonium salts of phosphorous acids was carried out on the basis of coke-chemical raw materials – the isoquinoline fraction, which is a mixture of quinoline, isoquinoline, toluidines and other heterocyclic compounds. A high degree of anticorrosion protection of the synthesized heterilonium salts of phosphorous acids is shown as corrosion inhibitors of oilfield equipment in aqueous media containing hydrogen sulfide and carbon dioxide.

An analysis of the literature on the synthesis and use of corrosion inhibitors shows that heterocyclic compounds including pyridine and its derivatives are used as the active component. The widespread use of pyridine and their derivatives is delayed due to the lack of convenient methods for their synthesis. The diverse methods available in the literature for the synthesis of heterocycles are multi-stage. In addition, the starting compounds for their synthesis are in many cases difficult to access.

Research Methods. We used chromium mass spectroscopy: an AgilentTechnology gas chromatography mass spectrometer GS6890 / MS5973N using a capillary column measuring 30 m × 0.25 mm with 5% phenylmethylsiloxane in dimethylsiloxane, the carrier gas was hydrogen, and the injector temperature was 280 °C, the temperature of the MS source is 230 °C, the temperature of the MS quadrupole is 180 °C, when programming the temperature of the column thermostat from 100 to 280 °C, the temperature rise rate is 10 °C min, the sample size is 1 μl, in the non-dividing mode, X-ray diffraction patterns of the catalysts were taken on a DRON-2 diffractometer (radiation Cukα-copper, speed 2 deg / min), Paulik-Paulik and Erdey derivatograph; in addition, standardized test methods and others were studied to determine the physicomechanical and technological properties.

Experimental part. Catalysts for the synthesis of heterocyclic compounds were prepared by suspending the active components with a carrier, followed by molding, drying, and calcining, some comparative characteristics of which are presented in Table 1. As a carrier, alumina hydrate PPP-33% was used, according to TU6.03714–78.

Table 1.– Comparative characteristics of the used catalysts

No.	The catalyst and its composition, wt.%	The duration of the run to regeneration, hours.	Performance, g/hour	Acetylene conversion,%	The composition of the organic layer of catalysis				
					Acetonitrile	Pyridine	2-methylpyridine	3 and 4-methylpyridine	By-products
1.	Cr_2O_3–20.0 Al_2O_3–80.0	24	92.0	94.0	92.0	–	traces	–	7.0
2.	ZnO-20.0 Al_2O_3–80.0	20	86.0	75.0	84.0	–	10.0	4.0	2.0
3.	CdF_2–20.0 Al_2O_3–80.0	48	102.0	92.0	20.0	–	48.0	24.0	18.0
4.	CdF_2–10.0 ZnO-5.0 Cr_2O_3–3.0 Al_2O_3–82.0	72	114	90.0	5.0	35.0	30.0	25.0	5.0
5.	CdF_2–5.0 ZnO-5.0 Cr_2O_3–5.0 AlF_3–3.0 Al_2O_3–82.0	96.0	110	93.0	7.0	–	51.0	26.0	16.0
6.	CdF_2–5.0 ZnO-5.0 Cr_2O_3–5.0 Fe_2O_3–3.0 AlF_3–3.0 Al_2O_3–78.0	144 180	120.0 135	95.0 96.0	3.0 5.0	35.0 traces	22.0 52.0	29.0 30	11.0 12.0

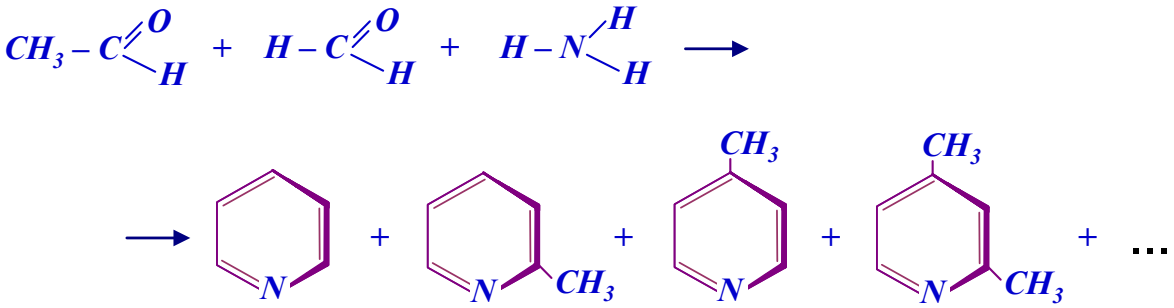

The heterocyclization of acetylene with ammonia (methanol) was carried out in a flow unit, in a stainless steel reactor with a size d × l = 25–1000 mm.

As the catalyst used catalyst № 6.

Individual products were isolated by fractionation of catalysis on a column with 30 t.t. and identified by their physical constants.

3-methylpyridine was isolated from a mixture of 3- and 4-methylpyridines by treating the latter with

formaldehyde, followed by steam distillation and azeotron distillation.

Results and discussion of research. The influence of the calcination temperature on the specific surface, productivity and conversion of catalyst No. 6 in the temperature range 450–650 °C was studied (Table 2).

Table 2.– Effect of calcination temperature on catalyst activity

Catalyst calcination temperature, °C	Specific surface area, м²/г	Productivity, g/kg cat hour	Acetylene conversion,%
450	182.0	124.0	92.0
500	170.0	120.0	85.0
575	145.0	92.0	70.0
650	102.0	70.0	55.0

As can be seen from the data (table 2), with an increase in the calcination temperature, the specific surface area and productivity of the catalyst gradually decrease, as well as the conversion of acetylene. With an increase in the calcination temperature from 450 to 650 °C, the $\gamma - Al_2O_3$ transition to $\alpha - Al_2O_3$ begins and pore sizes increase, which leads to a decrease in the specific surface.

When conducting thermal analysis of catalyst No. 6 on derivatograms, 3 endo- and 2-exothermic effects are distinguished (Fig. 1):

90–140 °C – endothermic effect of removal of capillary and adsorbed water;

180–220 °C – exothermic effect of crystallization of amorphous aluminum hydroxide;

240–290 °C – endothermic effect of thermal decomposition of hydroxysols of aluminum, zinc and cadmium;

310–340 °C – exothermic effect of the onset of crystallization of aluminum oxide;

440–460 °C – endothermic effect of the removal of structural hydroxides from the crystal lattice of aluminum oxide and the occurrence of solid-phase reactions with the formation of solid solutions.

In connection with the studies of the thermal synthesis of catalysts, we note that, with an increase in the operating time of catalyst № 6, a significant increase in the mechanical strength of the catalyst (by 12 kg/cm² in 200 hours) was found with a simultaneous decrease in its specific surface (from 151.6 to 97.2 m²/g).

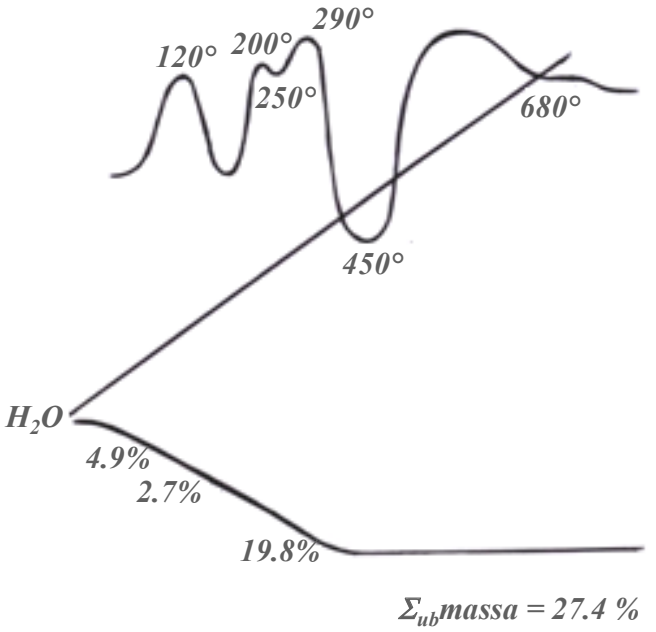

Figure 1. Catalyst Derivatogram № 6

This is most likely due to the fact that, as the operating time of the catalyst increases, a new crystalline phase is released. All investigated samples of the catalysts in the fresh state were amorphous, the formation of the crystalline phase was observed only after 150–200 hours of operation.

The study of the porous structure of the catalyst samples showed that all the studied samples are characterized by the presence of small pores in them. The pore sizes of the studied catalysts range from 40–50, and their pore volume is in the range of 0.3–0.15 cm³/g.

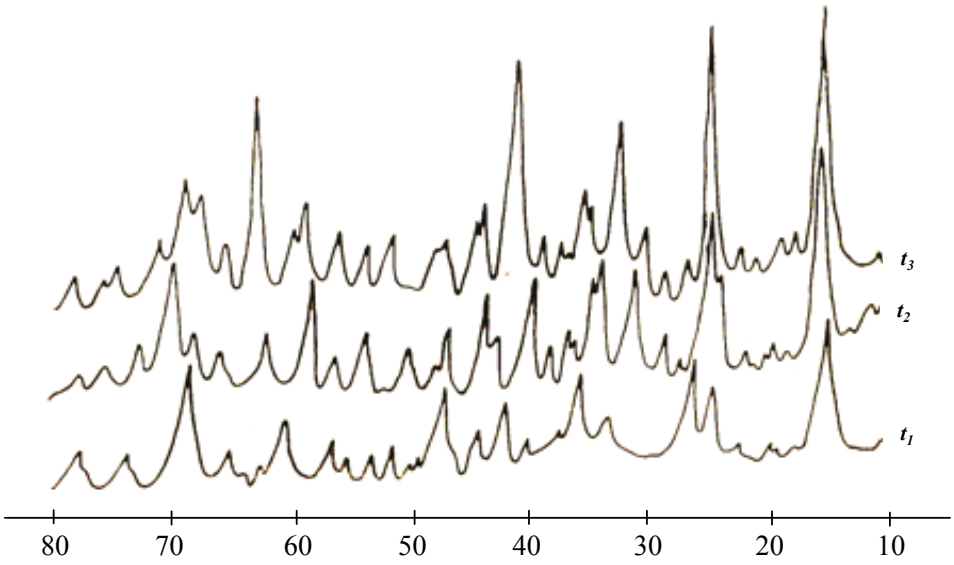

Figure 2. X-ray diffraction patterns of catalyst No. 6 calcined at various temperatures: t_1 = 500 °C; 2. t_2 = 575 °C; 3. t_3 = 650 °C

X-ray studies showed that the catalysts have a fairly high activity in the polyamorphic-crystalline state when chemically bound water is retained. With an increase in the calcination temperature from 450 to 650 °C, the fraction of the crystalline phase increases, the amount of chemically bound water decreases, the decomposition of hydroxy-fluorides begins, as a result of which the specific surface area of the catalyst decreases and its activity decreases (Fig. 2).

Table 3. – Effect of inhibitor mixture concentration on corrosion rate steel St. 3 in 15% acid (t = 60 °C, τ = 4 h)

Inhibitor concentration, mg/l	Corrosion Rate, g/m³·h	Protective action
No additives	131.0	–
0.2	6.5	95.0
0.4	4.6	96.9
0.6	4.0	98.2
0.8	2.0	99.0
1.0	1.4	99.5
1.2	2.3	98.6
B-3 (reference)	2.4	98.0

Table 4. – The effect of temperature on the corrosion rate and the protective effect of the inhibitor during corrosion of steel St.3 in 15% hydrochloric acid. Inhibitor's concentration is 0.8%

No.	Hydrochloric acid solution	Corrosion rate g/m² h	Protective effect,%
1	*2*	*3*	*4*
Room temperature. τ = 24 hours			
1	No additives	4.7	–
	With inhibitor	1.4	71.0
Temperature 40 °C. τ = 4 hours			

1	*2*	*3*	*4*
2	No additives	46.2	–
	With inhibitor	0.5	99.0
Temperature 80 °C. τ = 4 hours			
3	No additives	131.0	–
	With inhibitor	2.0	98.0
Temperature 100 °C. τ = 1 hours			
4	No additives	1020	–
	With inhibitor	4.9	99.5

When a mixture of acetylene (methanol) with ammonia is passed through, mainly pyridine mono derivatives (MSP-1) are formed in the catalysis, the mixture of which was tested as a corrosion inhibitor (tables 3–6).

At can be seen from the data in (table 3), the inhibitor effectively protects steel from corrosion at additive concentrations of 0.8–1.0%.

Table 5. – The effect of inhibitors on steel corrosion of strength grade D in a hydrogen sulfide medium. Room temperature. The concentration of hydrogen sulfide is 3.5–3.1 g/l. Medium – gas condensate: water = 1: 2. Stirring, 72 hours

Inhibitor	**Inhibitorconcentration, g/l**	**Corrosion rate g/m² hour**	**Degree of protection,%**
No additives	–	1.15	–
MSP-1	0.4	0.013	98.9
MSP-1	0.3	0.014	98.6
MSP-1	0.25	0.016	97.8
I-1-A (standard)	0.4	0.035	96.9

Table 6. – The effect of the MSP-1 series inhibitors on the corrosion of steel of strength grade D in a carbon dioxide environment (P_{CO_2} =1.0 MPa room temperature)

Inhibitor	**Inhibitor concentration, g/l**	**Corrosion rate g/m² hour**	**Degree of protection,%**
MSP-1	0.2	0.137	96.28
MSP-1	0.3	0.172	96.46
MSP-1	0.4	0.138	96.0
I-1-A (standard)	0.3	0.121	97.17

Conclusion. The catalytic reaction of producing pyridine and its derivatives by passing a mixture of acetylene (methanol) and ammonia was studied. The composition of the catalyst was selected, the influence of the calcination temperature on the specific surface, productivity and conversion of the catalyst was studied. It was found that with an increase in the calcination temperature from 450 to 650 °C, the $\gamma - Al_2O_3$ transition to $\alpha - Al_2O_3$ begins and pore sizes increase, which leads to a decrease in the specific surface, the catalysts have a rather high activity in the polyamorphic-crystalline state when chemically bound water is retained.

It was found that when a mixture of acetylene (methanol) with ammonia is passed through, mainly pyridine mono derivatives are formed in the ca-

talysis, whose protective effect upon corrosion of steel St.3 in 15% hydrochloric acid at a concentration of 0.8% is 99.5%.

References:

1. Shidota T. Jsces report jn the cost corrosion in Japan. Corcos. Manad. 2001.– No. 40.– P. 17–21.
2. Юсупов Д., Турсунов М. А., Хамраев Б. Н. Разработка новых реагентов для добычи нефти и газа. Химическая технология. Контроль и управление, 2007.– No. 1.– С. 38–39.
3. Мустафив Ф. М., Быков Л. И., Гумеров А. Г. и др. Зашита трубопроводов от коррозии.– Т. 2.– СПб.: Недра, 2007.– 708 с.
4. Колобова И. В. Гетероароматические основания и их комплексы с солями переходных металлов в качестве ингибиторов коррозии: дисс. … канд.техн.наук.– Уфа, 2006.– 115 с.
5. Медведева М. Л. Коррозия и зашита оборудования при переработке нефти и газа.– М: Изд-во Нефть и газ РГУ нефти и газа, 2005.– 312 с.
6. Можаров А. В., Цыганкова Л. Е., Иванов Е. С. Ингибирование углекислотной коррозии и наводороживания стали Ст 3. // Химия и хим. технология 2002.– Т. 45. Вып.6.– С. 157–162.
7. Моисеева Л. С., Тур Ю. Ю., Рашевская Н. С. // Практика противокоррозионной защиты. 2002.– No. 1 (23).– С. 30–41.

https://doi.org/10.29013/AJT-20-3.4-46-51

Nazarov Shomurod Komilovich,
intern applicant chemistry department
of Bukhara Engineering Technological Institute
Olimov Bobur Bahodir,
coal trainee intern applicant chemistry department
of Bukhara Engineering Technological Institute
Akhmedov Vohid Nizomovich,
Ph.D., Associate Professor, Department of Chemistry,
Bukhara Engineering Technological Institute
E-mail: voxid7@mail.ru

ELECTRONIC STRUCTURE AND QUANTUM-CHEMICAL CALCULATIONS OF VINYL ESTERS OF PHENOLS

Abstract. To date, methods of quantum-chemical calculations have been increasingly developed. As a result, it is possible to estimate the geometry of molecules, calculate the stability of intermediate products and transition states. In the experimental method of calculating such results for most reactions, along with a multi-stage process, there are difficulties associated with the appearance of intermediate stages and the presence of intermediate reaction products in an extremely small time.

Keywords: semi-empirical methods, RM3 and AM1, 3D-structure, hydroquinone, resorcinol, mono-vinyl ethers.

As is known, physical-chemical properties and reactivity of molecules are related to their electronic structure and energy features [1].

The rapid development of quantum-chemical calculation methods and the emergence of powerful computer tools allowed to determine many properties of complex organic substances. Therefore, in quantum-chemical and molecular-dynamic research, in obtaining information necessary for creating certain patterns and mechanisms of synthesis of organic compounds, these methods of physical-chemical research are of particular importance [2].

Quantum chemistry makes it possible to explain experimental data on the reaction activity of organic compounds and predict possible reactions. The basis of modern quantum chemistry is the Schrödinger equation, which is usually solved for stationary states in the adiabatic process [3].

Using methods of quantum chemistry it is possible to obtain data on electronic density, distribution of electronic density, the potential fields of reaction and various spectroscopic calculations. Currently, quantum chemistry techniques are the cheapest, simplest, and most versatile methods of studying the electron structure of molecules. However, it is not possible completely abandoning traditional experimental methods of studying substances. Since traditional methods take into account all external factors. Due to the complex nature of the substances, it is necessary to take into account the influence of temperature, the nature of the solvent, catalysts, etc. [4; 5].

The activity of the molecule in all reactions depends largely on its electronic structure and energy properties. With the development of quantum-chemical methods of computational, chemists have

the opportunity to plan experimental works and perform targeted synthesis of products.

Based on this, the electronic structure of the vinyl ethers of phenols used in the research was studied, as well as quantum-chemical calculations were carried out. The results obtained for the spatial geometry and the electron structure of phenol molecules using semi-empirical RM3 and AM1 methods were summarized and illustrated by resorcinol, hydroquinone and their vinyl ethers (Fig. 1–2).

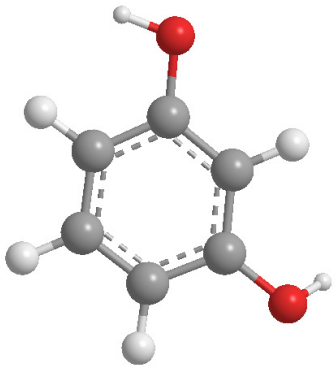

Figure 1. 3D-structure of the resorcinol molecule

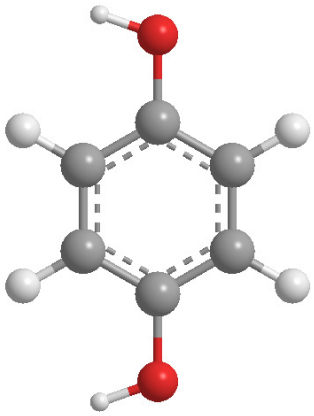

Figure 2. 3D structure of the hydroquinone molecule

The distribution of charges in atoms in the molecules studied shows that the oxygen atom in the hydroxyl group of the initial material molecules has a high negative charge value. Consequently, the vinylation reaction under the reaction conditions studied in hydroxyphenols takes place by their hydroxyl group (Fig. 3–6).

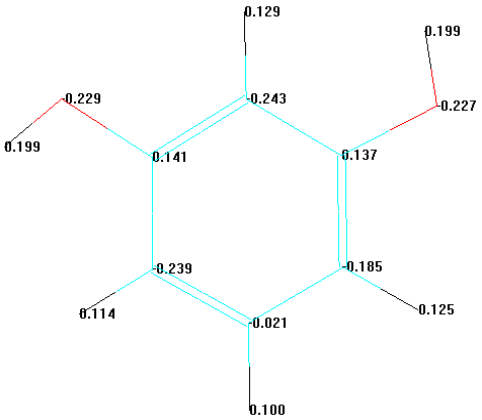

Figure 3. Charge distribution in atoms in resorcinol molecule

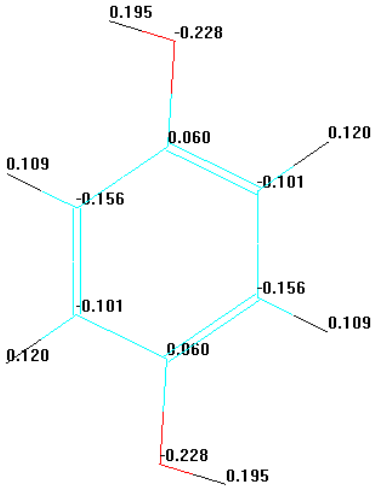

Figure 4. Charge distribution in atoms in the hydroquinone molecule

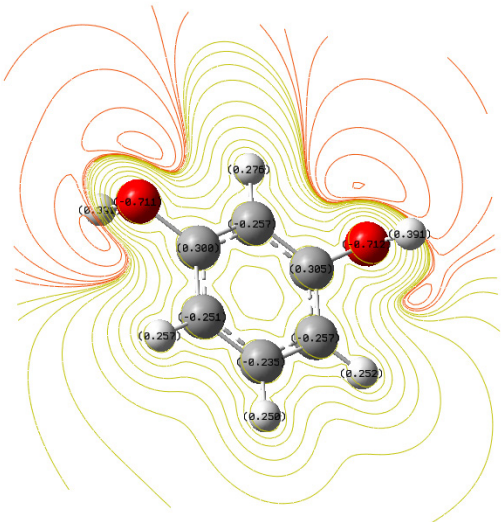

Figure 5. Electron density distribution in resorcinol molecule

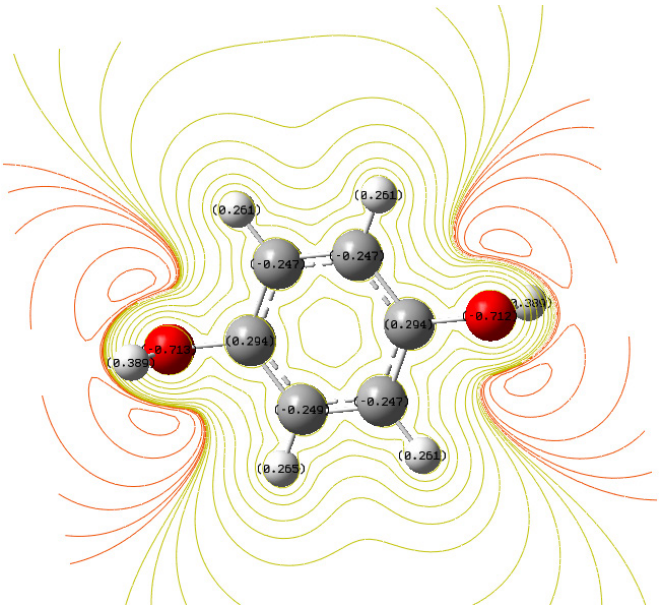

Figure 6. Electron density distribution in the hydroquinone molecule

This fact indicates that the hydroxyl group in the initial material composition, due to the high electron-negative oxygen of the hydroxyl group, the electron cloud distribution is relatively dense and is the reaction center where the electrophilic reagent can be attached, due to the vinylation reaction occur in these centers. For a more detailed description of the substances and their use as a database, quantum-chemical calculations of synthesized vinyl compounds were also performed (Fig. 7–9).

The quantum chemical calculations of the substances selected for the vinylation process were studied, and the results were presented in Table 1. The electronic structure and energy properties of the selected molecules (total energy, formation energy, heat of formation, electron energy, core energy, dipole moment, and oxygen atom charge) allow analyzing the molecules of aromatic phenol and pre-determining their reaction center.

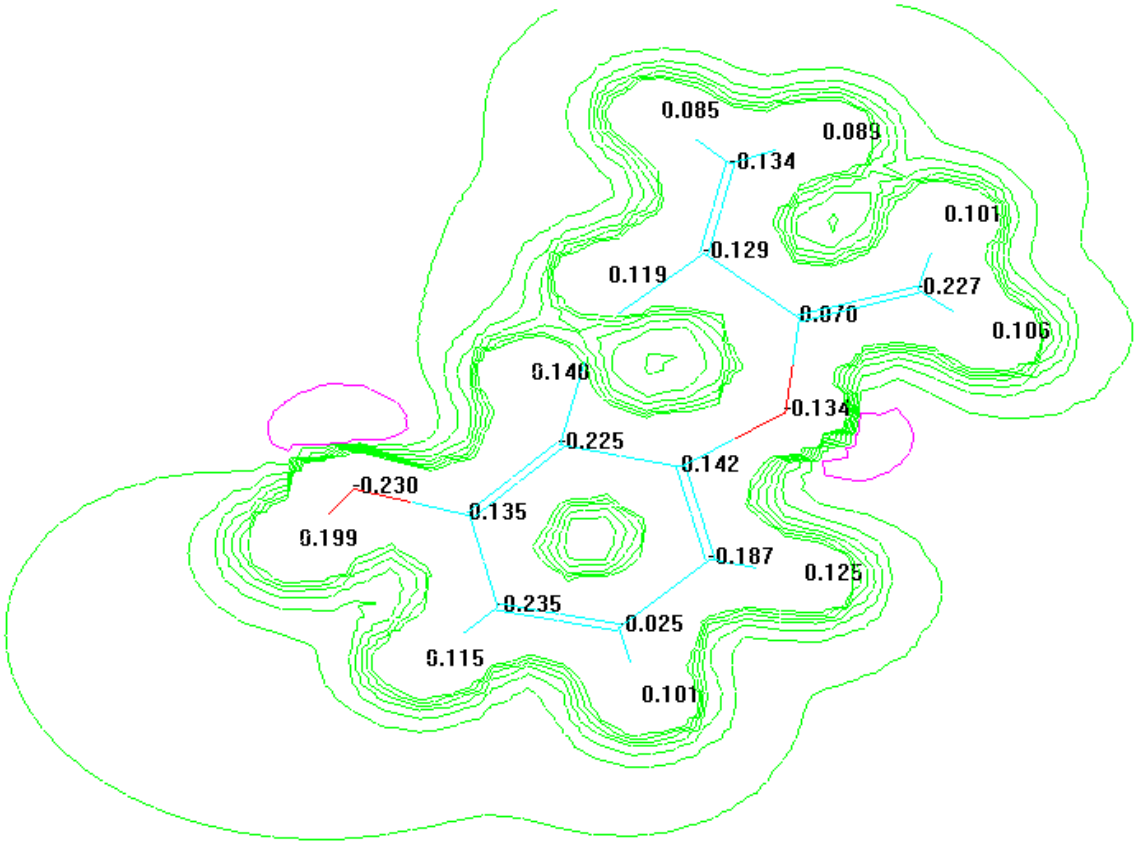

Figure 7. Distribution of electron densities in resorcinol monovinyl ester molecule

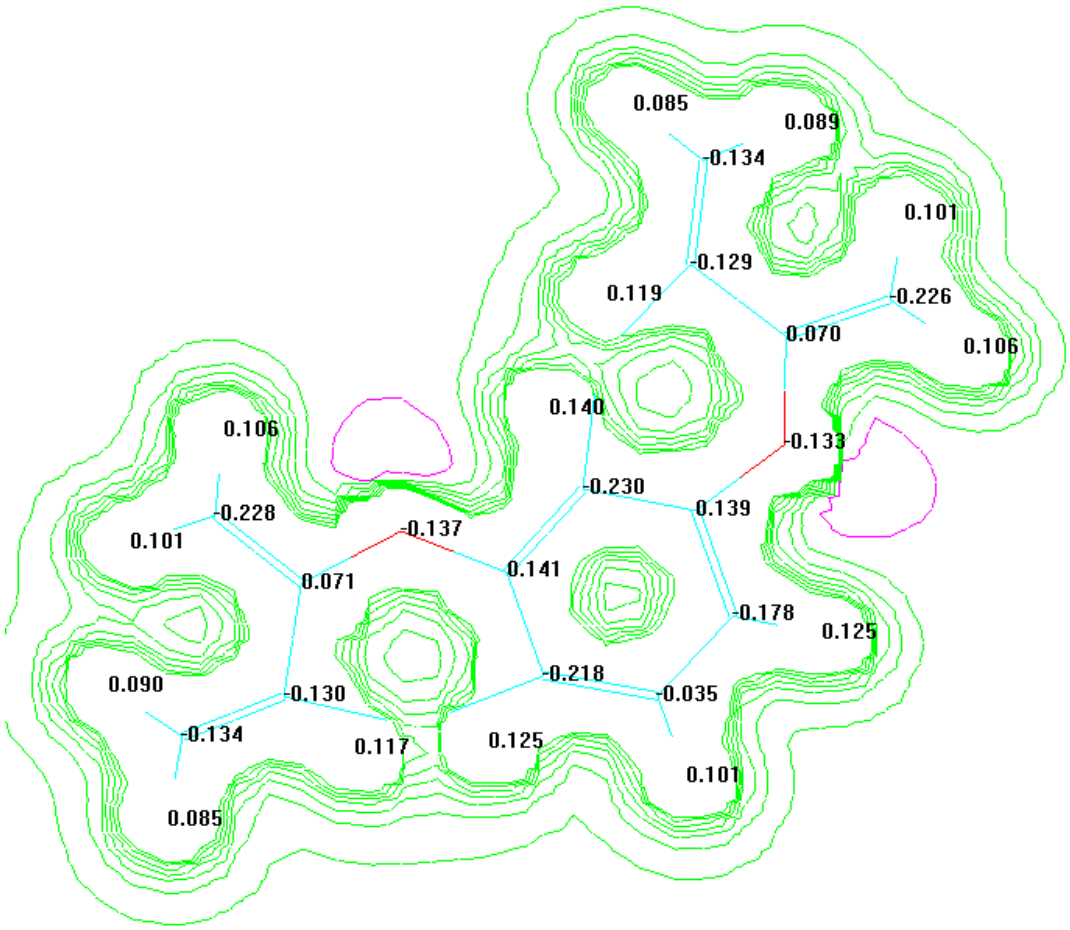

Figure 8. Distribution of electron densities in resorcinol ether divinyl molecule

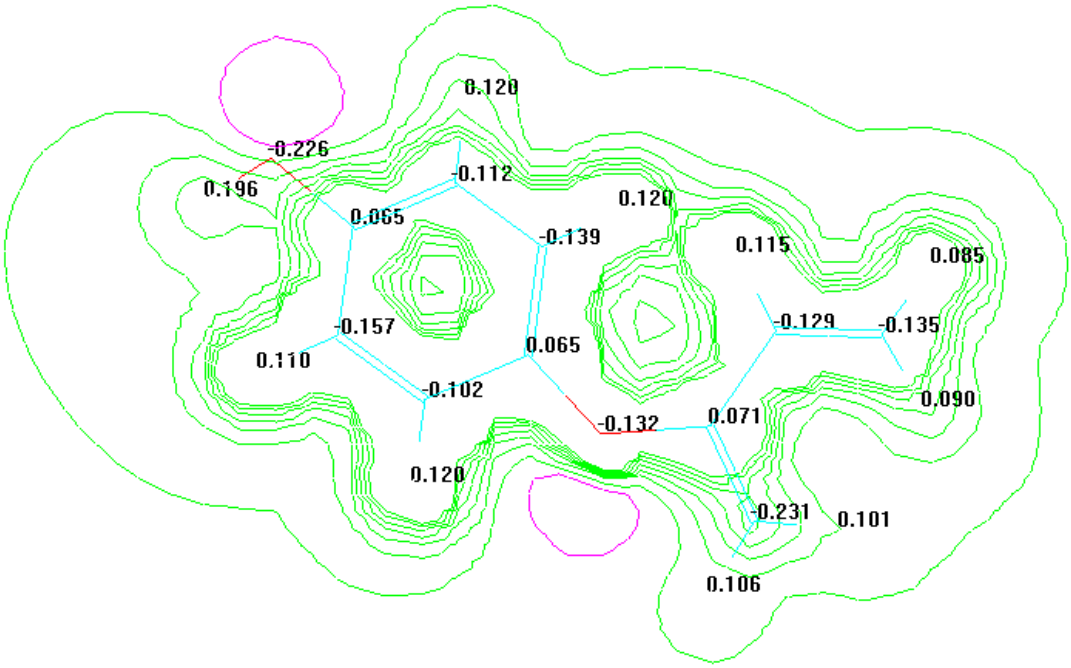

Figure 9. Distribution of electron densities in the hydroquinone monovinyl ester molecule

Table 1.– Quantum chemical calculations of the compounds used

Compounds	Total energy, kcal/mole	Formation energy, kcal/ mole	Formation heat, kcal/ mole	Electron energy, eV	Core energy, kcal/ mole	Dipole moment (D)	Oxygen atom charge
Initial substances							
Vinylacetylene	–12291.9	–825.7	66.266	–36325.86	24033.95	0.1485	–
Hydroquinone	–32067.66	–1523.33	–66.255	–129407.22	97339.56	0.00299	–0.456
Resorcinol	–32068.86	–1524.52	–67.456	–129756.3	97687.44	1.119	–0.456
Synthesized vinyl compounds							
Resorcinol monovinyl ether	–44371.06	–2360.52	–11.48	–227953.15	183582.08	0.9639	–0.364
Resorcinol divinyl ester	–56673.17	–3196.41	44.591	–341301.17	284628	1.159	–0.27
Hydroquinone monovinyl ether	–44370	–2359.45	–10.42	–226372.85	182002.84	0.124	–0.358

Conclusion

Carrying out quantum-chemical calculations of initial chemicals, carrying out mathematical modeling of obtained results is important in planning chemical reactions, especially in determining technological parameters of reactions and development of technologies.

In this article, quantum-chemical calculations of used initial materials and formed compounds were carried out: the spatial 3D-structure of the molecule, the distribution of charges and electron density in the atoms of the molecule, the total energy of the molecule, the energy of formation, the heat of formation, the energy of the electron, the energy of the nucleus, the dipole moment and the important charge of the oxygen atom were determined. Based on the analysis of the results, the scientific hypothesis is that the vinyl process is caused by oxygen of the hydroxyl group, which was confirmed by the results of experiments and based on spectral analysis. The results obtained are presented in the form of an iconogram, a diagram and a table.

References:

1. Parmanov A. B., Nurmonov S. E., Kolesinsko Beata, Mavloniy M. I., Khandamov B. N. Synthesis of vinyl ethers of aromatic carbonic acids based on vinyl acetate // Uzbekistan chemistry journal, – Tashkent 2019.– No. 4.– P. 42–47.
2. Parmanov A. B., Nurmonov S. E., Kolesinsko Beata, Khandamov B. N. Synthesis of vinyl esters of carboxylic acids with the participation of 2-chloro-4,6-dimethoxy-1,3,5-triazine // International conference "Youth as a driving force for the development of science", – Chimkent, Kazakhstan, 2019.– P. 183–185.
3. Nurmanov S. E., Soliev M. I., Mirhamitova D. Kh. Electronic structure of aromatic acetylene alcohols and modeling of their vinylization // "Modern research and innovation" Journal.–Moscow. 2015.– No. 3.– P. 43329–43385.
4. Mirkhamitova D. K., Urazov Sh. M., Zakirova Sh. Quantum-chemical calculations of organic substances on the basis of modern information technologies // Republican scientific and technical conference

on innovative technologies in designing, construction and operation of engineering communications, Fergana, 2019.– March, 29–30.– P. 274–276.

5. Mirkhamitova D. Kh., Sirlibaev T. S., Sharipov Sh. Electronic structure, quantum-chemical calculations of some amines and mathematical modeling of their vinylization // Herald of National University of Uzbekistan.– Tashkent, 2009.– No. 3.– P. 155–159.

https://doi.org/10.29013/AJT-20-3.4-52-54

Ruzieva Komila Ernazarovna,
Senior Lecturer, Bukhara Engineering
and Technology Institute, Bukhara, Uzbekistan
E-mail: b_sspo_devon@mail.ru

FUNCTIONS AND PRINCIPLES OF MEASUREMENTS IN PEDAGOGICAL DIAGNOSTICS

Abstract. The article provides methods for measuring functions and principles in pedagogical diagnostics. The analysis of measurements in the field of diagnostics is given and the methods and components of these measurements will be substantiated.

Keywords: measurement, interpretation, non-physical measure, methodological connection, scale, formal-conceptual approach, epistemological aspect, axiomatization, formalization.

Introduction. Measurement is the most common procedure in everyday life. We measure the distance from work to home, the growth of a person, the amount of food we want to eat, the mood of our co-talk, the pleasure of a conversation, the beauty of nature or photographs, that is, almost all our life is unimaginable [1; 2; 5; 7].

The dimension came with human civilization and became an integral part of human life.

Initially, the measurement was the most elementary in its construction and demonstrated the calculations of many objects of the same type based on a comparison of the number of fingers. In turn, the size of the objects was compared with the length of the fingers, feet, or steps. Thus, the principle of quantum fusion was invented – the separation of phenomena into separate elements (quanta). Years, thousands of years have passed, and advances in science and technology have allowed people to develop methods that can be measured in various fields of knowledge [3; 4].

To understand what a measurement is, we look at different types of measurements or different interpretations of the concept of "measurement".

Physical measurements are usually performed in two ways:

1) There are a number of experiments that give us digital data that help us determine not only the nature (quality), but also the size (number) of observed changes. Most physical measurements are a measure of length, because the measuring line determines the position of strings, threads, light indices, or liquids. The measured value is determined by the distance from zero, that is, the length.

2) The measurement includes three elements: an object or system for work; a system that is monitored and compared, and the specifications for this operation.

Methodologically, the physical size is determined as follows:

– measurements are taken on real objects that are not related to the object of knowledge;

– an empirical procedure for determining numerical values using measuring instruments is necessary, which is associated with observation and experiment, assuming the observed properties of the measurement object;

– definitions in the form of observable characteristics (quality) and quantity (quantity) of measurement objects, on the other hand, the main elements of measurements, on the other hand, quantitative and qualitative values. The measurement procedure allows you to specify the numerical values of the properties measured using the data of the measuring tool, using the appropriate unit of measurement, which coincides with the measuring device.

The measurement process is based on comparing the measured property with a unit of measurement.

Continuing our thoughts, we are trying to portray a non-physical dimension.

This type of measurement consists of two components: a measuring device that is easy to understand and very easy to use, and personal measurements that will be presented or used to evaluate the object.

The non-physical dimension is nothing more than a classification of a thing or event that allows each particular group to assign a specific symbol.

When we compare physical and non-physical dimensions, the non-physical dimension is associated with a person's personal qualities, his feelings, desires and relationships, that is, those attributes that are not suitable for the physical dimension.

A distinctive feature of a non-physical measure is its methodological connection with the classification of a non-physical measure. If the physical measurement is associated only with observation and experience, then in some cases the non-physical measurement can be both observational and experimental [6; 7].

Any measure assumes the existence of the subject and the result of the measurement as a condition, but in non-physical dimensions, the numerical characteristics of the properties of the object, as a result, act.

The measurement operation itself, unlike physical measurements, is not defined. Many sources relate to measuring instruments, as well as measuring instruments, observations, questionnaires, interviews, and so on. If the scales in the physical scale relate to the scale of measuring devices, the scale for non-physical measurements is conceptual, it means representing measurable results of any kind, at any level. In other words, the scale becomes a tool.

The most systematic measurement problem is in his works N. R. Campbell gives different definitions of the concept of "measurement":

– metric – "assignment of numbers to represent properties";

– measurement is "the process of assigning numbers to express adjectives";

– measurement is "to give numbers to show characteristics in accordance with scientific laws";

– the measure is to "give things in numbers so that they reflect facts or agreements about them."

All these definitions are essentially the same – measurement is a process of numbers.

Based on the numerical purpose of measurement, N. Campbell laid the foundations of the theory of representative measurements. The numerical result, according to this theory, allows us to draw important conclusions about the specific characteristics of the measurement object, taking into account certain rules and procedures.

Campbell's interest in measurement problems has led to the emergence of various theories and methods of measurement. The formal-conceptual approach found supporters in the person of Scott and Suppes. One of the most popular definitions of measurement is given by J. Glass and J. Stanley in his book, Statistical Methods in Pedagogy and Psychology. It makes no sense to publish all the works of American or English teachers and psychologists, as well as publications that have a "dimension" – a dimension.

It is clear that measurement is objectively limited, and it is clear that the quantitative characteristics of objects, events, and processes can serve as limitations. This objective basis of measurement refers to the level of knowledge, practical requirements and technological capabilities achieved.

There is no doubt that the measurement is one of the most important scientific procedures at the present time, and its importance with the development of the humanities is becoming increasingly apparent.

However, it should be remembered that the mathematics of any science is not spontaneous, but a way of obtaining new information on the topic of research.

Any use of quantitative methods, mathematical models, axiomatization and formalization cannot replace the development of fundamental theoretical concepts.

The epistemological aspect of measurement as a cognitive method is that it is part of practical activity and is inseparable from it. Thus, as the basis of socio-pedagogical diagnostics, which is part of pedagogy and, in turn, part of a certain universe, the measure is subject to certain general rules.

References:

1. Campbell N. R. Les Principes de la Physique, 1989.– 200 p.
2. Glass J., Stanley J. Statistical methods in pedagogy and psychology. 1995.– 288 p.
3. Vygotsky L. S. Pedagogical psychology.– M., 1996.– 287 p.
4. Winter I. A. Pedagogical psychology.– M.: Logos, 2002.– 162 p.
5. Educational psychology. Ed. N. V. Klyueva.– M.: Vlados-Press, 2003.– 255 p.
6. Petrovsky V. A. Psychology of education.– M., 1995.– 312 p.
7. Talyzina N. F. Pedagogical psychology.– M., Vlados, 1998.– 378 p.

https://doi.org/10.29013/AJT-20-3.4-55-58

Yakhshieva Zukhra Ziyatovna,
Doctor of Chemistry, Professor
Kalonov Rustam Mamadierovich,
Teacher, Djizakh State Pedagogical Institute
named after A. Qodiriy, Uzbekistan
E-mail: yaxshiyeva67@mail.ru
Khudaiberdieva Umida Ermatovna,
chemistry teacher of general education school
No. 12 in Pakhtakor City, Jizzakh Region, Uzbekistan
Muyassarova Kumush Ikrom,
Kizi, third-year student
of Djizakh State Pedagogical Institute, Uzbekistan

ASPECTS OF APPLICABILITY OF DIETHYLDITHIOCARBAMATE SALTS IN ANTIMONY TITRATION

Abstract. The paper shows aspects of applicability of carbamates and optimizes the conditions for amperometric titration of antimony with a solution of lead diethyldithiocarbamate with two platinum indicator electrodes in media having different acid-base properties relative to the current of anodic oxidation of reagent and cathodic reduction of titrated metal ions. During experiment, the metrological characteristics (reproducibility, correctness, band extension of determined contents, sensitivity, selectivity) were improved, the fields of use of the antimony titration method were expanded with a view to their subsequent application when controlling the composition of natural objects and industrial materials.

Keywords: amperometric titration, electrochemistry, selectivity, reproducibility, reagent, selectivity, expressivity.

Introduction. Increased requirements for analytical composition control of poorly water-soluble organic objects at all stages of technological processes dictate increased requirements for accuracy, expressivity, selectivity and expansion of the range of determined contents of analysis methods developed or implemented in production. The most accurate ways to indicate the endpoint of titration include electrochemical methods, in particular, amperometric methods with one or two polarized indicator electrodes.

Theoretical analysis. Lead diethyldithiocarbamate (Pb(DTC)2) forms together with many cations very sound and almost non-water-soluble complex compounds that can be extracted by many organic solvents (benzene, butanone, carbon tetrachloride, chloroform, etc.).

Trial experiments have shown that when titrating the antimony cation in protolytic media with two platinum indicator electrodes, clear curves are registered that allow to accurately find the position of equivalence point using a conventional graphical technique. Determination of a titration endpoint (TEP), regardless of the nature of solvent used, corresponds to the formation of complexes

in a molar ratio Me: ligand –1:3 for trivalent cation ions.

Experimental procedure. Amperometric titration with two platinum indicator electrodes, as follows from the current–voltage characteristic of Pb(DTC)2, should be performed at voltages below 0.5 V on the acetate background, 0,4 V on the nitrate background and 0,5 V on the perchlorate background, so that the processes of anodic titrant oxidation and cathodic oxygen reduction could simultaneously occur. If the voltage is too high and Pb(DTC)2 is used as a titrant, the current can also occur through anodic oxidation of lead ions formed during the reaction and cathodic oxygen reduction.

In order to optimize the titration conditions with Pb(DTC)2 solutions, the effect of external voltage magnitude applied to the indicator electrodes, the nature and concentration of background electrolyte, additives of an inert solvent, different foreign cations, interfering anions, a number of complexing compounds and other factors have been studied.

Results and discussion.

External voltage effect. In accordance with current-voltage characteristics of Pb(DTC)2, with antimony ions participating in complexation reaction, as well as dissolved oxygen, amperometric titration of metal ions with two platinum indicator electrodes on various background electrolytes should be performed at a voltage not lower than 0,30 V, so that after the equivalence point, the processes of anodic free reagent oxidation and cathodic oxygen reduction could simultaneously occur. Dimethylformamide dissolved oxygen starts to recover with a noticeable rate only at potentials of 0.35 V. The voltage was changed in the range of 0.3–1.1 V stepwise of 0.2 V.

Taking into account this circumstance, as well as indicated values of the half-wave potentials ($E_{1/2}$) of Pb(DTC)2 and the oxidation starting point of acetic acid, n-propanol, dimethylformamide or dimethylsulfoxydum it can be concluded that the amperometric titration of non-reducible cations upon platinum cathode should be controlled at a voltage of at least 0.8 V [1].

Experiments have shown that one gets the best-shaped curves and correct results of titration of metal ions when the indicator electrodes voltage is not lower than 0.9 V.

It was found that when the applied voltage is less than 0.4 V during amperometric titration with Pb(DTC)2 solution, the right ascending branch of a curve is too flat and quickly deviates from straightness, leading to a decrease in reproducibility of the curve shape and, consequently, to incorrect titration results.

The curve shape of amperometric antimony titration with Pb(DTC)2 solution is adequate to the curves obtained during its determination and to the equivalence point, cathodic antimony ions and anodic organic solvent oxidation will be reduced.

In order to get clearer curves of amperometric titration, the next experiments were performed with increased electrode voltage up to 0.9 V. At this voltage, the right branch of the curve becomes steeper and its area of smooth curvature is significantly reduced.

Effect of background electrolyte nature and concentration. Since the acid-base properties and concentration of the background electrolyte have a very significant effect on the curve shape, conditions and results of titration of metal ions, the effect of its nature and concentration has been studied in detail at a voltage of 0.5–0.8 V (depending on the nature of titrated medium). The effect of three background electrolytes: potassium acetate, nitrate and lithium perchlorate, that differ in their nature and exhibit basic, neutral and acidic properties, respectively, was studied.

Experiments have shown that the antimony titration with Pb(DTC)2 solution at background electrolyte concentration of 0.1–0.3 M proceeds relatively quickly, while the shape of titration curve, its preciseness and position of TEP basically do not change when concentration of the background electrolyte varies. If its concentration is too high (more than 0.5 M), the shape of amperometric titration curve gets worse: the right branch quickly loses its steepness

and linearity, the area of smooth transition between the branches increases, and the position of equivalence point shifts towards overestimation. If the background concentration is too low because of the low electrical conductivity of the analyzed solution, the right branch of titration curve becomes curved and TEP, although slightly, is shifted in the direction of overestimation [2; 3].

Antimony titration with lithium nitrate is slightly faster than with potassium and ammonium acetate. The titrant demand at TEP changes in proportion to the amount of antimony added, but the equivalence point position does not exactly correspond to the stoichiometry of normal metal thiocarbaminate formation, as it occurs when titrating this cation on the acetate background. At the same time, one antimony atom accounts for two reagent molecules, that is, mixed-ligand complexes are formed. It should be emphasized that this ratio of 1:3 components in the complex was seen with a solution of Pb(DTC)2 in glacial acetic acid.

Experiments have shown that amperometric titration of antimony with a solution of Pb(DTC)2 proceeds quickly enough and on an acetate background only, and it was impossible to get sufficiently reproducible and correct results with nitrate and lithium perchlorate. The titrant consumption at the equivalence point with potassium acetate is proportional to the amount of antimony taken. Changes in this background concentration in the range of 0.1–0.3 M has little impact on the curve shape and the results of antimony titration.

According to the observed data received during the titration of various metal ions, it can be concluded that the change in the concentration of the background electrolyte – potassium acetate or ammonium in the solution under study (0,03–0,04 M), the shape and preciseness of amperometric titration curve remains largely unchanged, however, if the background concentration is too high (more than 0.4 M), the determination results are noticeably high. If their concentration is too low (less than 0.2 M), the shape of titration curve is significantly deteriorated: its right branch becomes less steep and quickly loses its straightness, bending to the volume axis.

Thus, for amperometric titration of different metal ions (except for bismuth ions) with solutions of Pb(DTC)2, the best background electrolyte is considered to be potassium acetate with an optimal concentration in the range of 0.1–0.25 M [4].

Effect of the nature and concentration of inert solvent. In order to determine whether the proposed amperometric method with two indicator electrodes can be used for determining metal ions directly in extracts or in organic objects, the effect of carbon tetrachloride, chloroform, benzene and other solvents often and widely used as extraction agents on the conditions and results of titration with solutions of Pb(DTC)2 was studied. Titration was performed under optimal conditions, except that in the solution analyzed, one or another part of protolytic solvent was replaced with an inert solvent (from 10.0 to 50.0 vol.%).

Experiments have shown that carbon tetrachloride additives have least effect on the shape of curves and the results of amperometric titration of antimony. Even with its content of 40 vol.%, the titration results are still correct and reproducible. Hexane starts to overestimate the results of titration of metal ions at a content exceeding 35.0 vol.%, and chloroform and benzene – from 25.0 and 30.0 vol.%, respectively.

According to findings, when titrating Sb(III), Pd(II), Hg(II), Bi(III), Ag(I), Au(III) and other metals, the addition of increasing amounts of any of the studied non-aqueous solvents first markedly improves the shape of amperometric titration curve – its right branch becomes steeper, and the area of smooth curvature decreases, which indicates an increase in the effective stability constant (ESC) of the complex influenced by addition of inert solvent.

In addition, equilibration after each addition of the titrant is always significantly accelerated when its added to. Chloroform additives have a particularly favorable effect on the shape of titration curve.

However, starting from approximately 30–50 vol.% (depending on the solvent nature) of the added inert solvent, the steepness of the right branch of the titration curve continuously decreases as its content increases owing to decrease in the electrical conductivity of the solution under study. It should be noted that the sharpness of the amperometric titration curve slope after the equivalence point increases in all cases as the concentration of any of the studied inert solvent increases, indicating that the strength degree of the formed metal complex is increased [5–7].

Thus, based on our study, it can be concluded that the addition of small amounts of an inert solvent (not more than 30–40 vol.%) to protolytic solvents leads to a significant increase in the preciseness of the titration curve and, consequently, to an increase in the definition accuracy. The optimal content of an inert solvent that gives the best titration results depends on its nature. The most accurate value of this quantity is obtained for chloroform (45 vol.%), benzene (50 vol.%), and methyl ethyl ketone (40 vol.%).

It follows therefrom that it is best to perform amperometric titration of studied metal ions using benzene and chloroform extracts, since the best-shaped titration curves with less protolytic solvent are obtained at their presence.

Conclusion. Thus, the proposed method for titration of antimony ions with a solution of Pb(DTC)2 has quite satisfactory accuracy and speed of analysis.

References:

1. Геворгян А. М., Талипов Ш. Т., Хадеев В. А., Мухамеджанова Д. В. Вольт-амперометрическое поведение диэтилдитиокарбамината натрия на платиновом аноде в среде диметилформамида // Журн. аналит. химии. 1980.– Т. 35.– № 10.– С. 2026–2028.
2. Лурье Ю. Ю. Справочник по аналитической химии.– М.: Химия. 1979.– С. 230–236.
3. Фишер Р. А. Статистические методы для исследователей, занимающихся определением благородных элементов.– М.; Мир. 1988.– 287 с.
4. Геворгян А. М., Яхшиева З. З., Киреев Г. В. Комплексонометрическая амперометрия при определении благородных металлов в объектах окружающей среды. Тез. докл. Респ. научно–прак. конф. «Кимёнинг долзарб муаммолари» – Самарканд. 2009.– С. 65–66.
5. Геворгян А. М., Талипов Ш. Т., Хадеев В. А., Мирзоян И. И. Вольтамперные кривые окисления тионалида на платиновом микроаноде в ледяной уксусной кислоте // Депонир. в ВИНИТИ № 4616–81 от 24.09.81.– С. 1–3.
6. Геворгян А. М., Яхшиева З. З., Жураева Л. К., Рахимбердиева Г. У. Определение числа электронов, отдаваемых при электроокислении одной молекулы тиомочевины // Республиканская научно-практическая конференция с международным участием «Зеленая химия» – в интересах устойчивого развития.– Самарканд. 2012.
7. Yakhshieva Z. The conditions for amperometric titration of the Ag (I) ion with sulfur-containing reagents. // Universia Chemistry and Biology. Electronic scientific journal. 2016.– No. 4(22).

Contents